Self-assembly patterns of non-metalloid silver thiolates: structural, HR-ESI-MS and stability studies

Anastasia V. Chupina,[a] Vadim V. Yanshole,[b,c] Veronica S. Sulyaeva,[a] Vasily V. Kokovkin,[a] Pavel A. Abramov,*[a] Maxim N. Sokolov [a]

[a] Nikolaev Institute of Inorganic Chemistry SB RAS, 3 Akad. Lavrentiev Ave., 630090 Novosibirsk, Russia;
[b] Novosibirsk State University, 2 Pirogova Ave., 630090 Novosibirsk, Russia;
[c] International Tomography Center, Institutskaya str. 3a, 630090, Novosibirsk, Russia;

Supporting information

Table of contents

Synthesis

^{t}BuSAg was prepared according to the standard reaction between $AgNO_3$ and ^{t}BuSH in CH_3CN in the presence of Et_3N. All reagents were of commercial quality and were used as purchased. IR spectra were recorded on a FT-801 FT-IR spectrometer (Simex, Russia). Elemental analysis was carried out on a Eurovector EA 3000 CHN analyser.

$[NO_3@Ag_{20}(^tBuS)_{10}(NO_3)_9(DMF)_6]$ (1): 0.015 g (0.076 mmol) of ^{t}BuSAg was added to the clear solution of 0.100 g (0.589 mmol) $AgNO_3$ in 5 mL of DMF. The dissolution of silver mercaptide is completely proceed during one hour under stirring at room temperature (25 °C). The resulting solution was transferred to diethyl ether atmosphere. A few days later a crop of colorless crystals was collected and dried in air. Yield: 0.013 g (42% based on ^{t}BuSAg).

IR (ATR, cm^{-1}): 2936 (w), 2856 (w), 1637 (vs), 1409 (s), 1386 (s), 1366 (s), 1303 (s), 1274 (vs), 1153 (s), 1100 (m), 1062 (w), 1031 (m), 938 (w), 864 (w), 807 (m), 722 (w), 662 (m).

Calc. for $[Ag_{20}(tBuS)_{10}(DMF)_6(NO_3)_{10}]$ C, H, N, S (%): 16.9, 3.2, 5.4, 7.8; found C, H, N, S (%): 16.1, 3.0, 5.2, 7.8.

$[NO_3@Ag_{20}(^tBuS)_{10}(NO_3)_8(NMP)_8][NO_3@Ag_{19}(^tBuS)_{10}(NO_3)_8(NMP)_6]\}_2(NO_3)$ (**2**): 0.015 g (0.076 mmol) of ^{t}BuSAg was added to the clear solution of 0.100 g (0.589 mmol) $AgNO_3$ in 5 mL of N-methyl-2-pyrrolidone (NMP). Colorless crystalline product immediately precipitates. Yield: 0.015 g (47% based on ^{t}BuSAg).

IR (ATR, cm^{-1}): 2954 (m), 2892 (m), 1630 (vs), 1506 (w), 1459 (m), 1407 (s), 1366 (s), 1317 (s), 1302 (s), 1263 (vs), 1149 (vs), 1113 (m), 1028 (s), 986 (w), 928 (w), 813 (m), 750 (w), 659 (m).

Calc. for $[NO_3@Ag_{20}(^tBuS)_{10}(NO_3)_8(NMP)_8][NO_3@Ag_{19}(^tBuS)_{10}(NO_3)_8(NMP)_6]_2(NO_3)$ C, H, N, S (%): 20.9, 3.6, 5.3, 7.6; found C, H, N, S (%): 21.4, 3.6, 5.7, 7.6.

$[Br@Ag_{16}(^tBuS)_8(NO_3)_7(DMF)_3]\cdot 3DMF$ (3): 0.070 g (0.355 mmol) of ^{t}BuSAg was added to the clear solution of 0.100 g (0.589 mmol) $AgNO_3$ in 5 mL of DMF. After complete dissolution 0.019 g (0.059mmol) of NBu_4Br was added. The resulting white precipitate was filtered off. The final solution was placed into a closed vessel with diethyl ether atmosphere. A crop of colorless crystals was collected and dried in air in several days. Yield: 0.087 g (58% based on ^{t}BuSAg).

IR (ATR, cm^{-1}): 2932(w), 1974 (w), 1642 (vs), 1461 (m), 1399 (s), 1381 (s), 1366 (s), 1265 (vs), 1151 (s), 1102 (s), 1063 (m), 1029 (m), 809 (m), 662 (m), 557 (s).

Calc. for $[BrAg_{16}(^tBuS)_8(NO_3)_7(DMF)_3]\cdot 3DMF$ C, H, N, S (%): 18.0, 3.4, 5.9, 7.7; found C, H, N, S (%): 17.7, 3.4, 5.4, 7.6.

Structural data

SCXRD

Crystallographic data and refinement details for **1-3** are given in Table S1. The diffraction data were collected on a New Xcalibur (Agilent Technologies) diffractometer with MoK_α radiation ($\lambda = 0.71073$) by doing φ scans of narrow (0.5°) frames. Absorption correction was done empirically using SCALE3 ABSPACK (CrysAlisPro, Agilent Technologies, Version 1.171.37.35 (release 13-08-2014 CrysAlis171 .NET)). Structures were solved by SHELXT[1] and refined by full-matrix least-squares treatment against $|F|^2$ in anisotropic approximation with SHELX 2014/7[2] in ShelXle program.[3] The main geometrical parameters are present in Table S2. H-atoms of organic ligands were refined in calculated positions.

In the structure of **2** a lot of NMP molecules have positional disorder which avoids refinement of this parts in anisotropic approximation without RIGU restraints. The positions of highly disordered NMP solvent molecules were not located. The complex composition was found from elemental analysis.

In the structure of **3** counter NO_3^- anions and DMF molecules located in the voids between silver clusters were not refined. The SQUEEZE procedure[4] of PLATON program[5] gives 153.5e per formula unit. This can be approximated as 2 NO_3^- and 2.25 DMF molecules. This fully correlates with elemental analysis.

The crystallographic data have been deposed in the Cambridge Crystallographic Data Centre under the deposition codes CCDC 2072541 (**1**), 2072542 (**2**), 2072543 (**3**).

References

(1) Sheldrick, G. M. SHELXT – Integrated Space-Group and Crystal-Structure Determination. *Acta Crystallogr. Sect. A Found. Adv.* **2015**, *71* (1), 3–8.

(2) Sheldrick, G. M. Crystal Structure Refinement with SHELXL. *Acta Crystallogr. Sect. C Struct. Chem.* **2015**, *71* (1), 3–8.

(3) Hübschle, C. B.; Sheldrick, G. M.; Dittrich, B. ShelXle : A Qt Graphical User Interface for SHELXL. *J. Appl. Crystallogr.* **2011**, *44* (6), 1281–1284.

(4) Spek, A. L. PLATON SQUEEZE: A Tool for the Calculation of the Disordered Solvent Contribution to the Calculated Structure Factors. *Acta Crystallogr. Sect. C Struct. Chem.* **2015**, *71* (1), 9–18.

(5) Spek, A. L. Structure Validation in Chemical Crystallography. *Acta Cryst* **2009**, *65*, 148–155.

Table S1. Experimental details

	1	**2**	**3**
Chemical formula	$C_{58}H_{132}Ag_{20}N_{16}O_{36}S_{10}$	$C_{226.50}H_{459}Ag_{58}N_{46.40}O_{94.20}S_{30}$	$C_{41}H_{86}Ag_{16}BrN_8O_{18}S_8$
M_r	4107.79	12558.43	3041.48
Crystal system, space group	Monoclinic, $P2_1/n$	Triclinic, $P\bar{1}$	Monoclinic, $C2/c$
Temperature (K)	140	140	120
a, b, c (Å)	16.9481(9), 12.5260(7), 26.7721(13)	15.9769(4), 25.0801(4), 25.4499(4)	18.2444(5), 41.9711(12), 15.2141(6)
α, β, γ (°)	90, 92.723(4), 90	100.571(1), 101.461(2), 102.566(2)	90, 91.211(3), 90
V (Å^3)	5677.1 (5)	9477.2 (3)	11647.4 (7)
Z	2	1	4
μ (mm^{-1})	3.62	3.15	3.15
Crystal size (mm)	0.20 × 0.10 × 0.08	0.20 × 0.10 × 0.10	0.20 × 0.20 × 0.10
T_{min}, T_{max}	0.768, 1.000	0.897, 1.000	0.869, 1.000
No. of measured, independent and observed [$I > 2\sigma(I)$] reflections	31711, 13522, 8672	88057, 44174, 22283	31002, 13848, 8388
R_{int}	0.050	0.056	0.032
θ values (°)	θ_{max} = 29.5, θ_{min} = 1.8	θ_{max} = 29.5, θ_{min} = 1.9	θ_{max} = 29.6, θ_{min} = 2.3
$(\sin\theta/\lambda)_{max}$ (Å^{-1})	0.693	0.692	0.694
Range of h, k, l	$-19 \le h \le 21$, $-16 \le k \le 15$, $-36 \le l \le 27$	$-21 \le h \le 13$, $-34 \le k \le 33$, $-34 \le l \le 34$	$-24 \le h \le 22$, $-56 \le k \le 45$, $-16 \le l \le 19$
$R[F^2 > 2\sigma(F^2)]$, $wR(F^2)$, S	0.050, 0.089, 0.97	0.075, 0.201, 1.00	0.063, 0.210, 1.12
No. of reflections, parameters, restraints	13522, 617, 6	44174, 2006, 176	13848, 413, 1
Weighting scheme	$w = 1/[\sigma^2(F_o^2) + (0.0279P)^2]$ where $P = (F_o^2 + 2F_c^2)/3$	$w = 1/[\sigma^2(F_o^2) + (0.0838P)^2]$ where $P = (F_o^2 + 2F_c^2)/3$	$w = 1/[\sigma^2(F_o^2) + (0.1066P)^2 + 1.1259P]$ where $P = (F_o^2 + 2F_c^2)/3$
$\Delta\rho_{max}$, $\Delta\rho_{min}$ (e Å^{-3})	1.83, -1.03	3.21, -1.38	1.51, -0.86

Computer programs: *CrysAlis PRO* 1.171.38.41 (Rigaku OD, 2015), *SHELXS2014* (Sheldrick, 2014), *SHELXL2014* (Sheldrick, 2014), ShelXle (Hübschle, 2011), CIFTAB-2014 (Sheldrick, 2014).

Table S2. Selected geometric parameters (Å)

1			
Ag1—Ag2	3.1459 (7)	S2—Ag7	2.4617 (16)
Ag1—Ag7^{i}	3.1662 (7)	S3—Ag3	2.4244 (15)
Ag1—Ag9^{i}	3.1239 (8)	S3—Ag5	2.5122 (16)
Ag2—Ag3	2.8980 (7)	S3—Ag8	2.4735 (15)
Ag2—Ag9^{i}	2.9193 (7)	S3—Ag10^{i}	2.4946 (15)
Ag2—Ag10^{i}	3.0964 (7)	S4—Ag1^{i}	2.6089 (17)
Ag3—Ag6B^{i}	3.322 (10)	S4—Ag7	2.4697 (16)
Ag3—Ag6A^{i}	3.0973 (11)	S4—Ag8	2.4440 (16)
Ag3—Ag10^{i}	3.1048 (7)	S4—Ag9	2.3788 (15)
Ag4—Ag5	3.0299 (7)	S5—Ag2^{i}	2.6183 (16)
Ag4—Ag10^{i}	3.0648 (7)	S5—Ag4^{i}	2.4699 (15)
Ag5—Ag7	3.0235 (7)	S5—Ag9	2.3853 (15)
Ag5—Ag8	3.0494 (7)	S5—Ag10	2.4971 (15)
Ag5—Ag10^{i}	3.0508 (7)	O1—Ag1	2.296 (5)
Ag6B—Ag7	3.125 (9)	O3—Ag2	2.350 (4)
Ag6A—Ag6B	0.623 (7)	O5—Ag2	2.558 (4)
Ag8—Ag9	3.2092 (7)	O6—Ag5	2.389 (4)
S1—Ag1	2.5217 (17)	O7—Ag7	2.584 (5)
S1—Ag2	2.5530 (16)	O8—Ag7	2.385 (4)
S1—Ag3	2.4254 (15)	O10A—Ag5^{i}	2.513 (9)
S1—Ag6B^{i}	2.353 (10)	O11—Ag10	2.308 (4)
S1—Ag6A^{i}	2.5765 (18)	O14B—Ag6A^{i}	2.577 (13)
S2—Ag4	2.4493 (16)	Ag6A—O18	2.261 (11)
S2—Ag5	2.5229 (16)	Ag6A—O19^{ii}	2.388 (10)
S2—Ag6B	2.344 (10)	Ag8—O17	2.546 (10)
S2—Ag6A	2.5282 (18)		
2			
Ag1—Ag2	3.0126 (12)	S7—Ag3	2.489 (3)
Ag1—Ag3	3.2429 (13)	S7—Ag20	2.419 (2)
Ag1—Ag21	3.0186 (13)	S7—Ag21	2.584 (3)
Ag2—Ag4	3.0752 (14)	S8—Ag1	2.527 (3)
Ag2—Ag21	2.9423 (13)	S8—Ag2	2.421 (3)
Ag2—Ag32	3.368 (11)	S8—Ag4	2.554 (3)
Ag4—Ag5	2.9008 (16)	S8—Ag5	2.678 (3)
Ag4—Ag7	3.1514 (13)	S8—Ag30	2.464 (12)
Ag4—Ag32	0.692 (9)	S8—Ag32	2.331 (11)
Ag5—Ag30	1.074 (13)	S9—Ag10	2.448 (4)
Ag5—Ag32	2.219 (10)	S9—Ag25^{iii}	2.559 (3)
Ag6—Ag8	2.9943 (12)	S9—Ag27	2.432 (3)
Ag7—Ag8	2.9896 (11)	S9—Ag28	2.543 (3)
Ag7—Ag9	3.1394 (12)	S10—Ag22^{iii}	2.593 (3)
Ag9—Ag12	3.1132 (13)	S10—Ag26	2.439 (4)
Ag9—Ag13	2.9696 (12)	S10—Ag27	2.433 (3)
Ag10—Ag11	3.2279 (14)	S10—Ag29	2.523 (4)
Ag10—Ag25^{iii}	3.0908 (14)	S11—Ag11^{iii}	2.601 (3)
Ag11—Ag22	3.229 (2)	S11—Ag24	2.433 (3)
Ag11—Ag25^{iii}	3.2949 (19)	S11—Ag25	2.532 (3)
Ag11—Ag26^{iii}	3.0227 (13)	S11—Ag26	2.434 (3)
Ag12—Ag13	3.0510 (11)	S12—Ag10	2.438 (4)
Ag13—Ag14	3.1102 (12)	S12—Ag11	2.536 (3)

Ag13—Ag15	3.2154 (14)	S12—Ag22	2.573 (4)
Ag14—Ag15	3.1258 (12)	S12—Ag23	2.440 (3)
Ag14—Ag18	3.2450 (14)	S13—Ag23	2.422 (3)
Ag15—Ag16	3.0982 (12)	S13—Ag24	2.451 (3)
Ag15—Ag17	3.2446 (16)	S13—Ag28^{iii}	2.608 (3)
Ag16—Ag17	3.1046 (13)	S13—Ag29^{iii}	2.590 (3)
Ag17—Ag18	3.1760 (13)	S14—Ag14	2.410 (3)
Ag17—Ag19	3.1507 (16)	S14—Ag15	2.578 (3)
Ag18—Ag19	3.2131 (15)	S14—Ag17	2.518 (3)
Ag19—Ag20	3.2556 (12)	S14—Ag18	2.413 (3)
Ag19—Ag21	3.2121 (14)	S15—Ag7	2.404 (3)
Ag20—Ag21	2.9972 (11)	S15—Ag9	2.566 (3)
Ag22—Ag23	3.1241 (15)	S15—Ag13	2.611 (3)
Ag22—Ag26^{iii}	3.2593 (17)	S15—Ag14	2.404 (3)
Ag22—Ag29^{iii}	3.1059 (18)	O1—Ag8	2.562 (8)
Ag23—Ag29^{iii}	3.1739 (17)	O2—Ag9	2.372 (8)
Ag24—Ag25	3.3224 (13)	O4—Ag8	2.311 (7)
Ag24—Ag28^{iii}	2.9717 (15)	O5B—Ag13	2.23 (3)
Ag25—Ag28^{iii}	3.1414 (18)	O8—Ag5	2.300 (11)
Ag27—Ag28	3.0432 (13)	O9B—Ag30	2.27 (2)
Ag27—Ag29	3.1965 (14)	O9A—Ag5	2.59 (4)
Ag30—Ag32	2.914 (16)	O9A—Ag30	2.36 (4)
S1—Ag3	2.440 (3)	O11—Ag1	2.275 (8)
S1—Ag5	2.451 (3)	O12—Ag21	2.515 (7)
S1—Ag6	2.387 (2)	O13—Ag21	2.366 (9)
S1—Ag30	2.475 (12)	O14—Ag19	2.491 (10)
S2—Ag4	2.504 (3)	O16—Ag19	2.252 (8)
S2—Ag7	2.428 (3)	O17—Ag17	2.540 (7)
S2—Ag8	2.512 (3)	O19—Ag15	2.353 (8)
S2—Ag32	2.291 (11)	O20—Ag20	2.583 (8)
S3—Ag6	2.442 (3)	O23—Ag16	2.582 (8)
S3—Ag8	2.592 (3)	O26—Ag4	2.498 (9)
S3—Ag9	2.526 (3)	O27B—Ag4	2.56 (3)
S3—Ag12	2.456 (3)	O29—Ag11	2.495 (11)
S4—Ag12	2.425 (2)	O31—Ag17	2.261 (17)
S4—Ag13	2.616 (3)	O33—Ag28	2.294 (11)
S4—Ag15	2.532 (2)	O34—Ag28	2.393 (15)
S4—Ag16	2.410 (3)	O35—Ag29	2.438 (17)
S5—Ag16	2.460 (3)	O37—Ag29	2.349 (12)
S5—Ag17	2.541 (3)	O38—Ag25	2.249 (10)
S5—Ag19	2.517 (3)	O39—Ag15	2.520 (11)
S5—Ag20	2.458 (2)	O40A—Ag13	2.383 (13)
S6—Ag2	2.430 (3)	O41—Ag3	2.460 (8)
S6—Ag18	2.403 (3)	O49—Ag11	2.367 (8)
S6—Ag19	2.604 (3)	O50—Ag29	2.23 (4)
S6—Ag21	2.598 (3)	O55—Ag22	2.346 (19)
S7—Ag1	2.496 (3)		
3			
Ag1—Ag2^{iv}	3.0365 (10)	S1—Ag3^{iv}	2.500 (2)
Ag1—Ag2	3.0365 (10)	S1—Ag9	2.410 (2)
Ag1—Ag3^{iv}	3.2996 (9)	S2—Ag2	2.435 (2)
Ag1—Ag3	3.2997 (9)	S2—Ag3	2.508 (2)
Ag2—Ag3	3.1272 (10)	S2—Ag4	2.488 (2)
Ag2—Ag5	3.2829 (9)	S2—Ag5	2.446 (2)

Ag2—Ag9	3.2851 (9)	S3—Ag5	2.455 (2)
Ag3—Ag4	3.3451 (11)	S3—Ag6	2.508 (2)
Ag3—Ag9^{iv}	3.1695 (11)	S3—Ag7	2.414 (2)
Ag4—Ag5	3.0248 (9)	S3—Ag8^{iv}	2.487 (2)
Ag4—Ag8^{iv}	3.1390 (11)	S4—Ag4^{iv}	2.518 (2)
Ag4—Ag9^{iv}	3.0585 (10)	S4—Ag7	2.409 (2)
Ag5—Ag7	3.1775 (9)	S4—Ag8	2.488 (2)
Ag5—Ag8^{iv}	3.0377 (10)	S4—Ag9	2.417 (2)
Ag6—Ag7^{iv}	3.2115 (10)	O1X—Ag6	2.254 (15)
Ag6—Ag7	3.2115 (10)	O2—Ag4	2.343 (13)
Ag6—Ag8^{iv}	3.3782 (9)	O3—Ag1	2.370 (14)
Ag6—Ag8	3.3783 (9)	O8—Ag8	2.310 (10)
Ag7—Ag8	3.0841 (10)	O14—Ag4^{iv}	2.47 (2)
Ag7—Ag9	3.3066 (10)	Ag3—O12B	2.21 (4)
S1—Ag1	2.499 (2)	Ag3—O12A	2.327 (13)
S1—Ag2	2.442 (2)	Ag5—Br1	2.9554 (7)

Symmetry code(s): (i) -*x*+1, -*y*+1, -*z*+1; (ii) -*x*+1, -*y*, -*z*+1; (iii) -*x*+1, -*y*+2, -*z*+1; (iv) -*x*+1, *y*, -*z*+1/2.

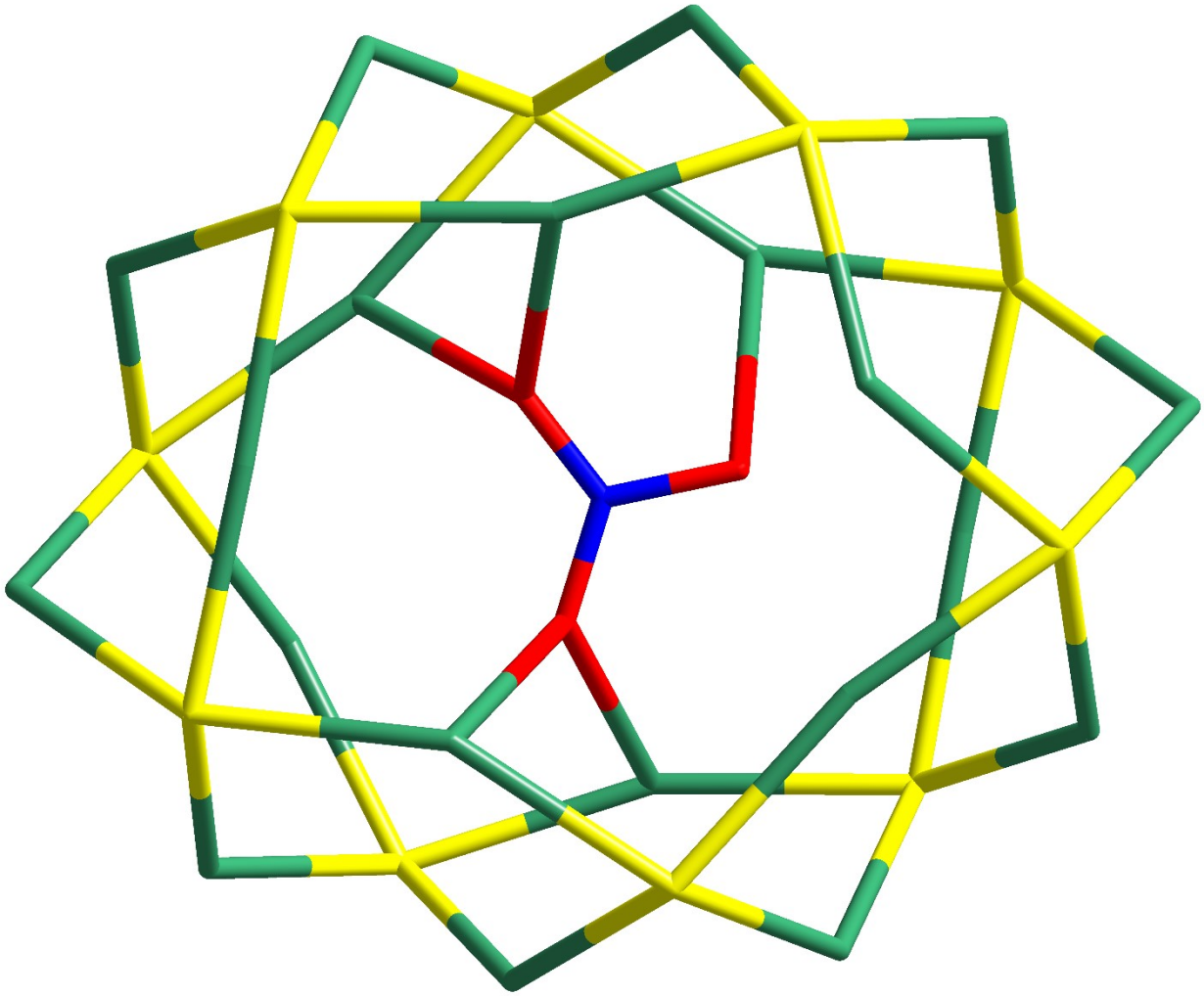

Fig. S1. The position of NO_3^- inside $\{Ag_{20}(tBuS)_{10}\}$ cluster core in the crystal structure of **1**.

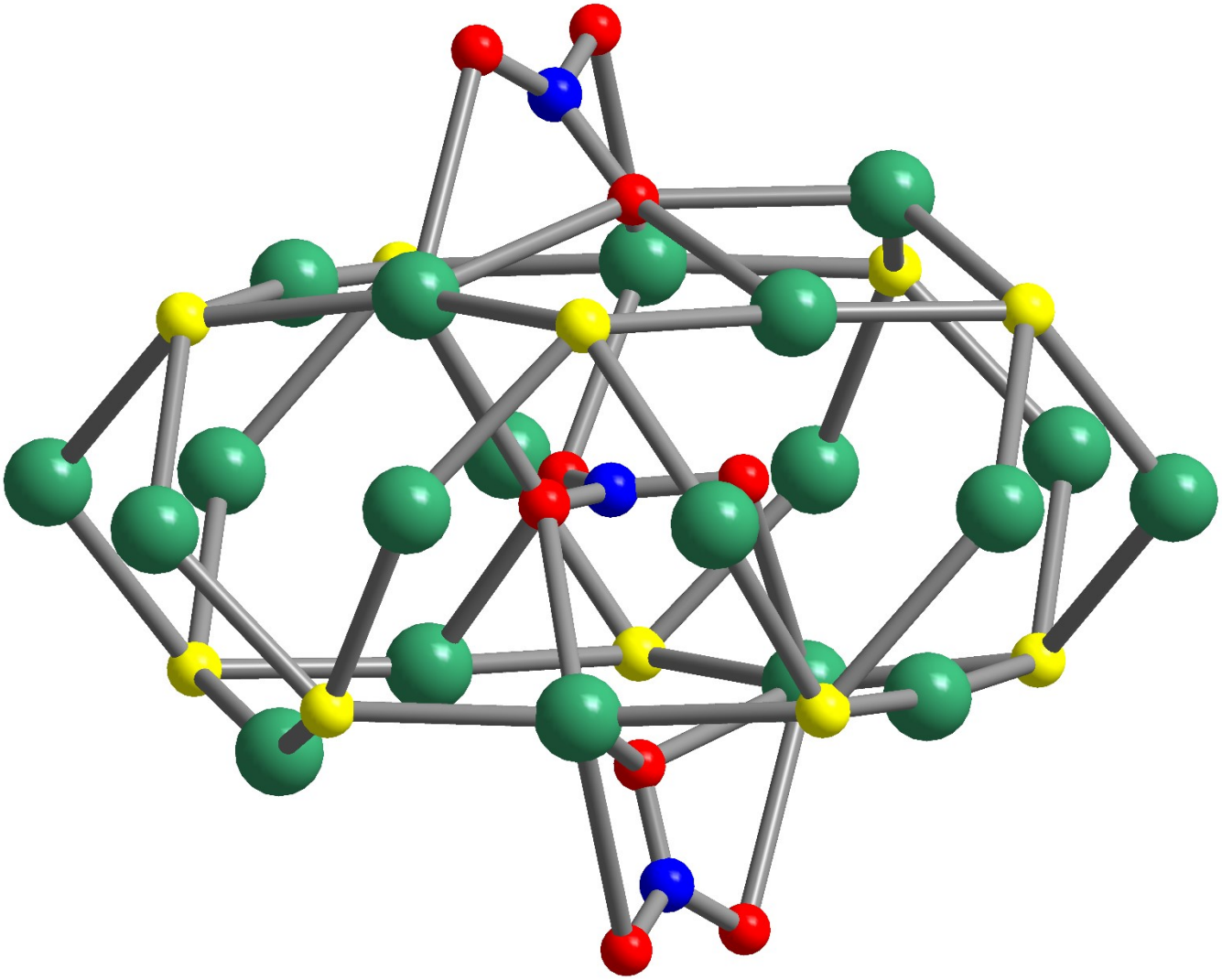

Fig. S2. The capping and central NO_3^- anions inside $\{Ag_{20}(tBuS)_{10}\}$ cluster core in the crystal structure of **1**.

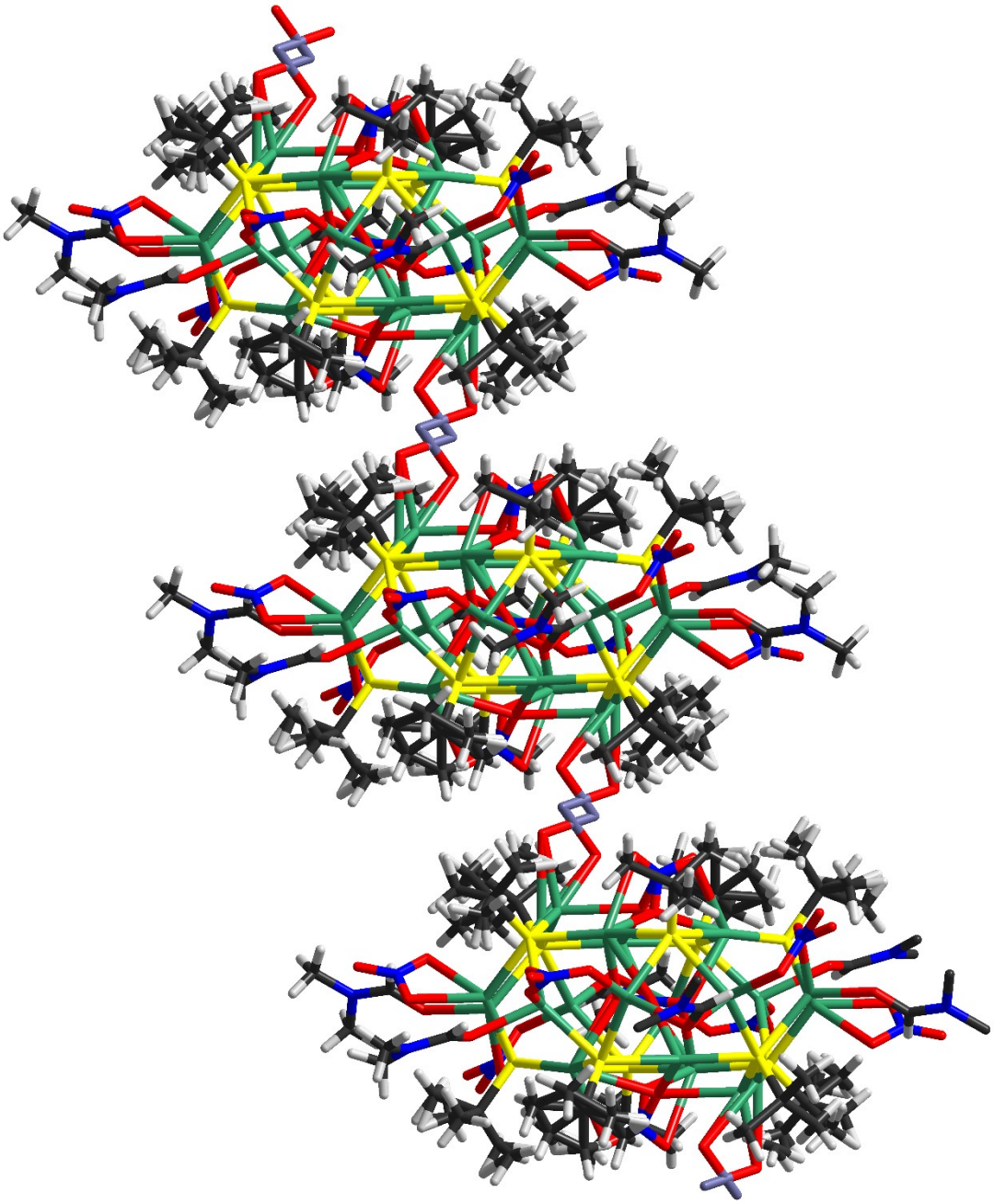

Fig. S3. The cluster chain fragment in the crystal structure of **1**.

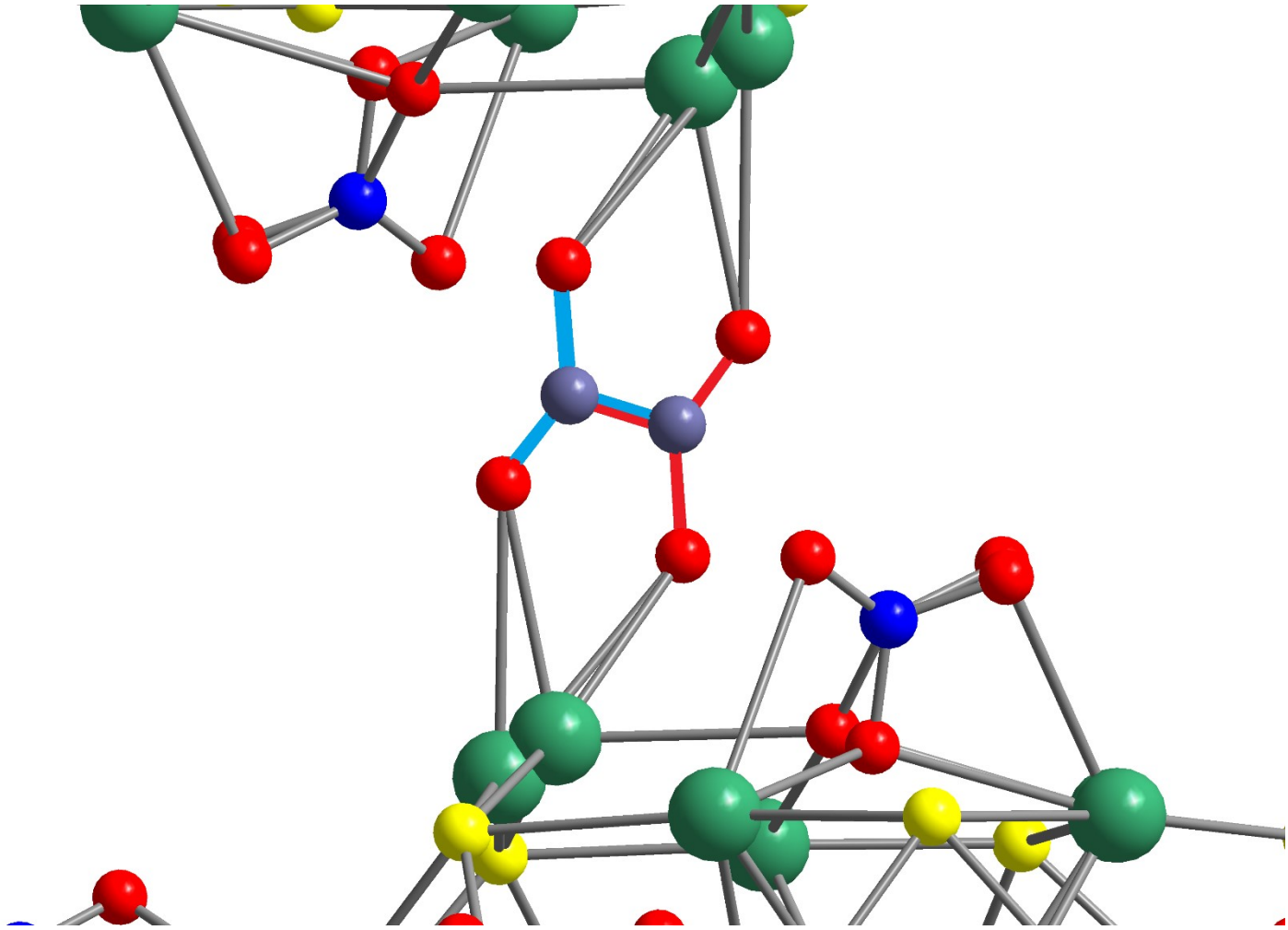

Fig. S4. Disordering of the bridged NO_3^- in the crystal structure of **1**.

Fig. S5. The FT-IR spectrum of **1**.

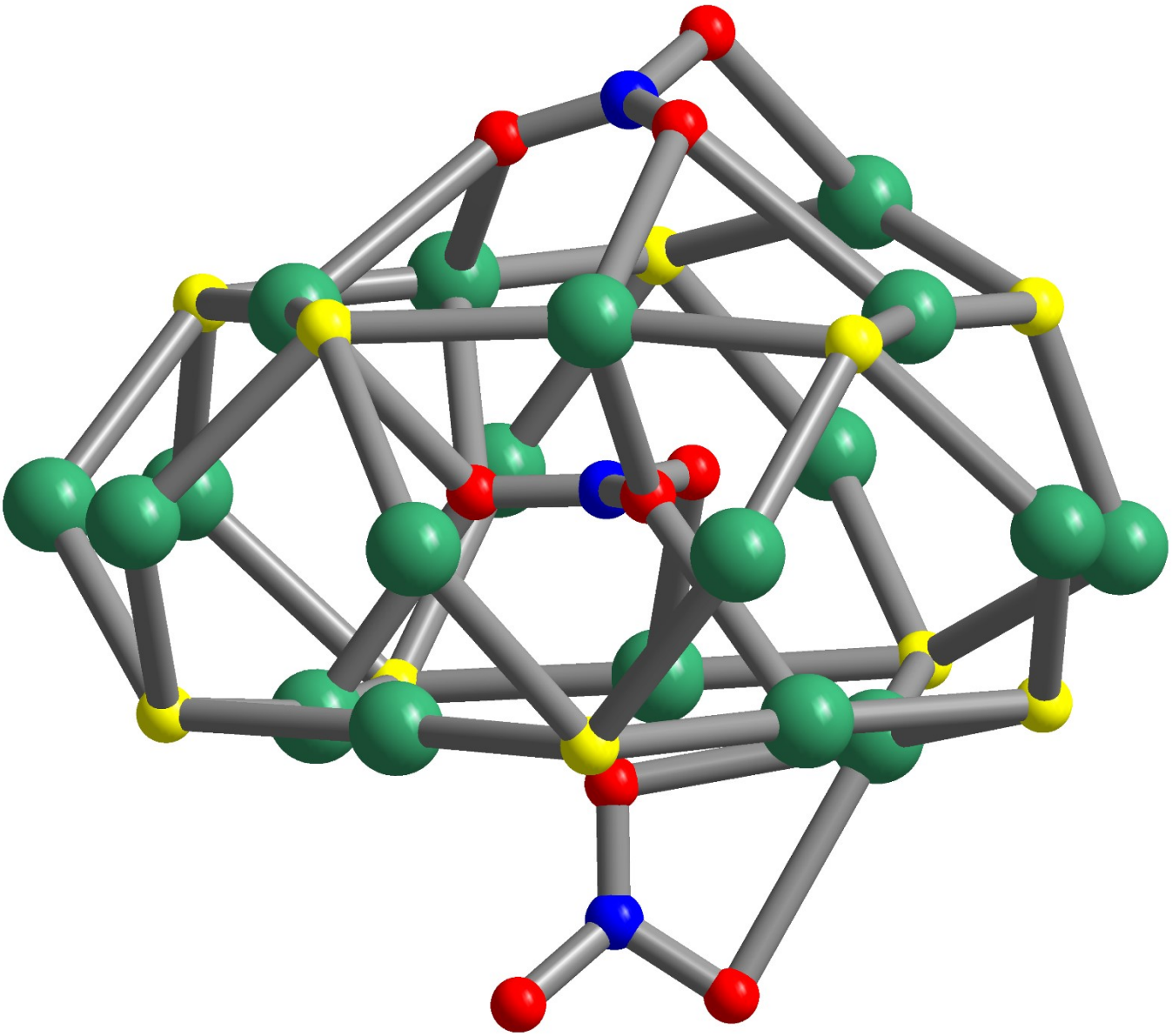

Fig. S6. The capping and central NO_3^- anions inside $\{Ag_{19}(tBuS)_{10}\}$ cluster core in the crystal structure of **2**.

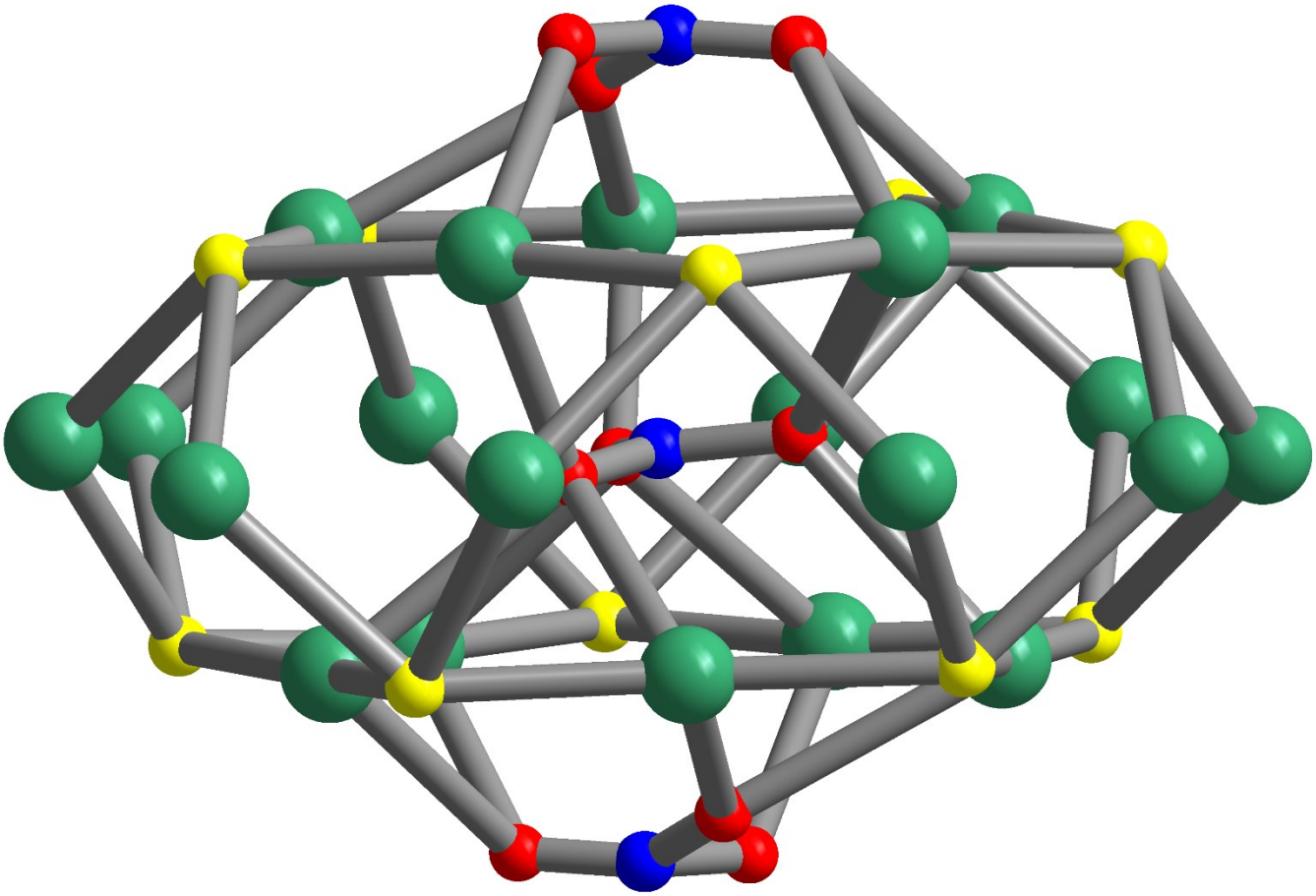

Fig. S7. The capping and central NO_3^- anions inside $\{Ag_{20}(tBuS)_{10}\}$ cluster core in the crystal structure of **2**.

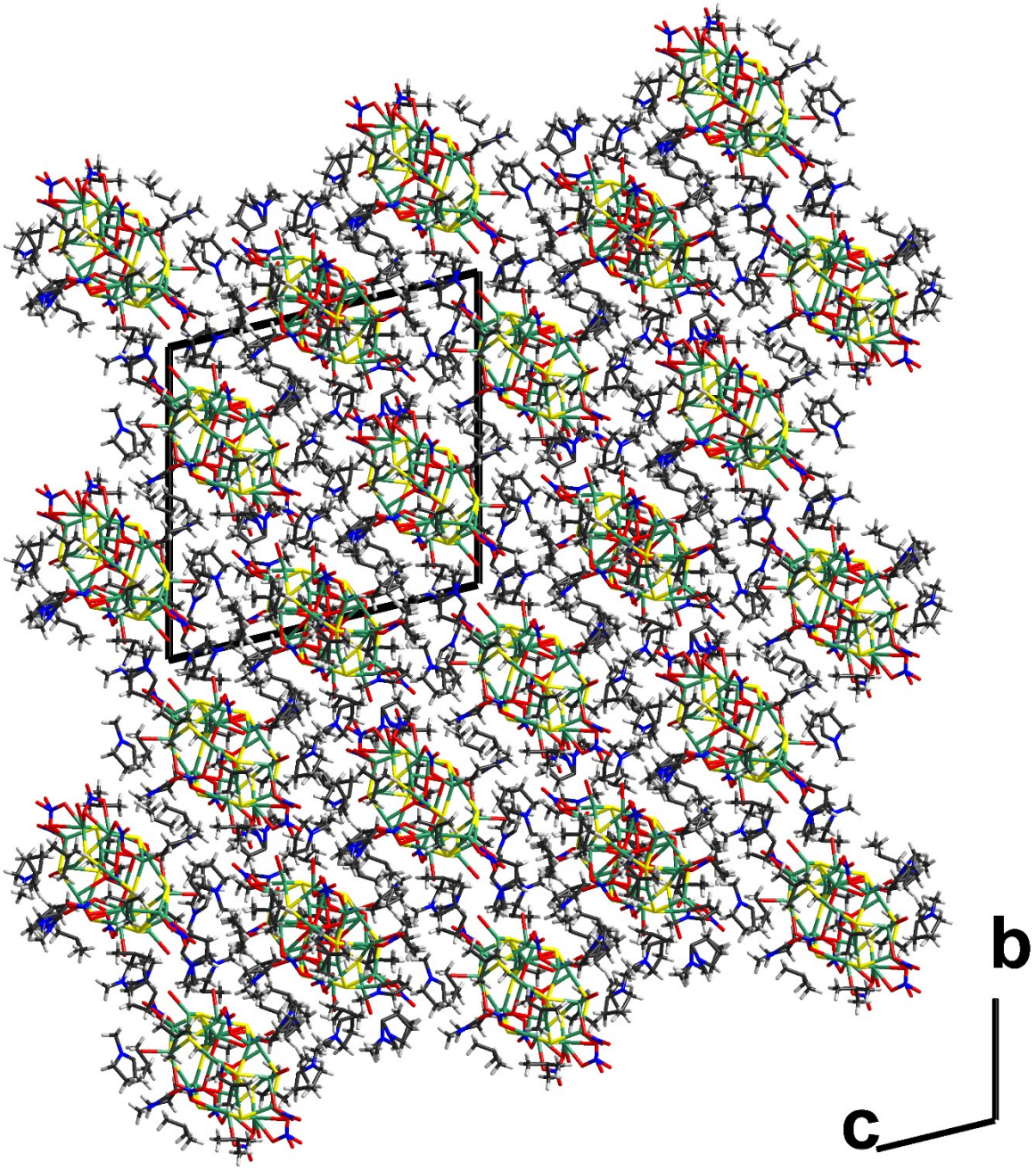

Fig. S8. The crystal packing of **2**.

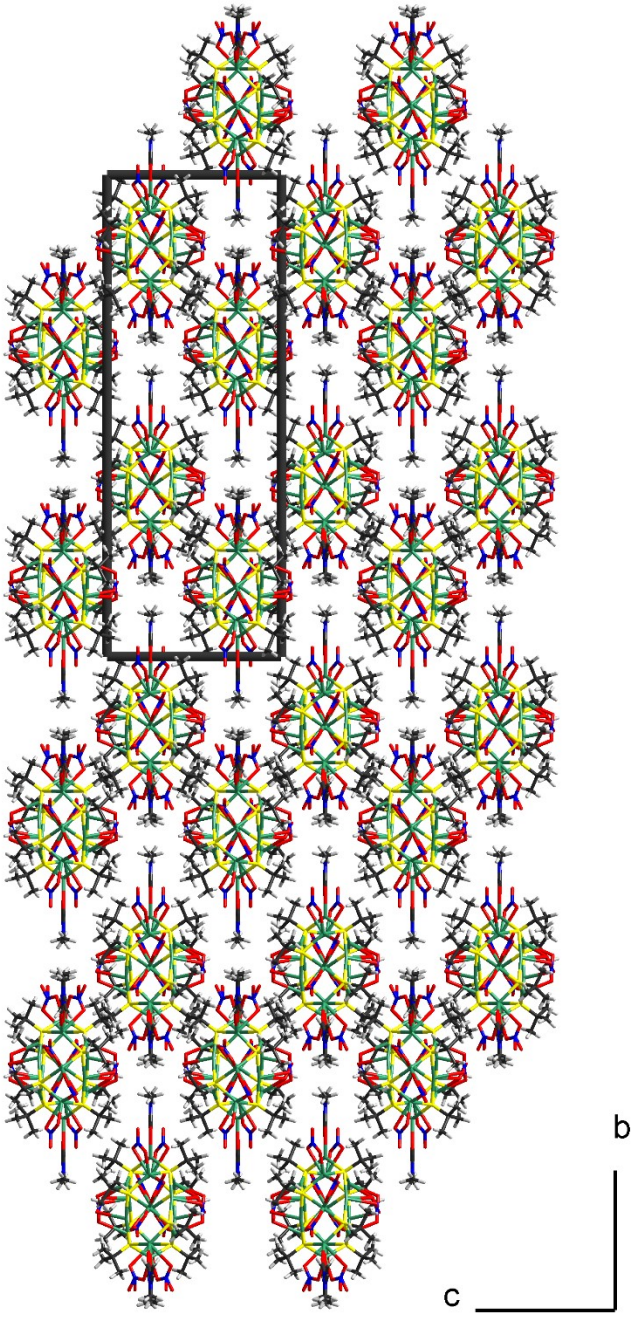

Fig. S9. Crystal packing of **3**. View along crystal axes *a*.

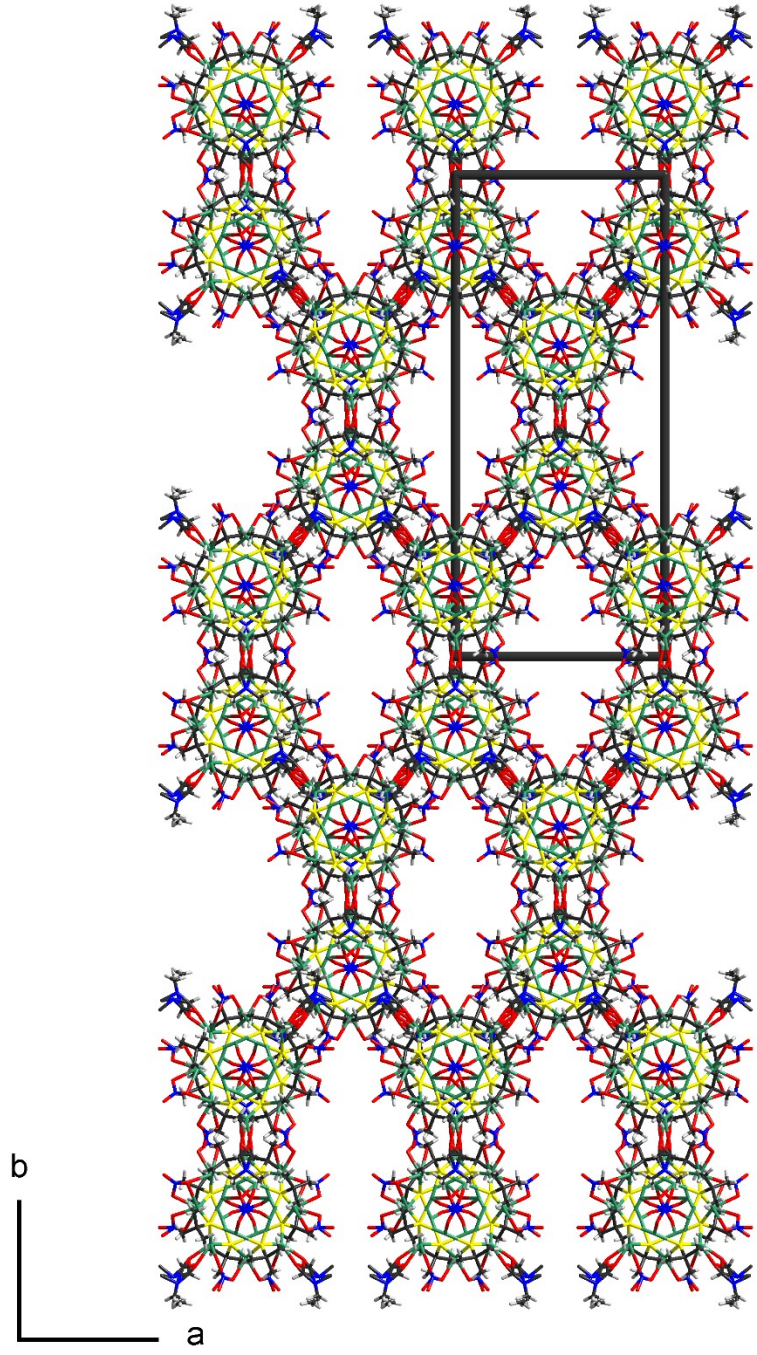

Fig. S10. Crystal packing of **3**. View along crystal axes *c*.

HR-ESI-MS data

The high-resolution electrospray ionization mass spectrometric (HR-ESI-MS) measurements were performed at the Center of Collective Use «Mass spectrometric investigations» SB RAS. Spectra were obtained with a direct injection of liquid samples on an ESI quadrupole time-of-flight (ESI-q-TOF) high-resolution mass spectrometer Maxis 4G (Bruker Daltonics, Germany). The spectra were recorded in the 300-3000 m/z range in negative and positive modes.

Fig. S11. Full HR-ESI-MS(-) spectrum of **1** in CH_3CN solution.

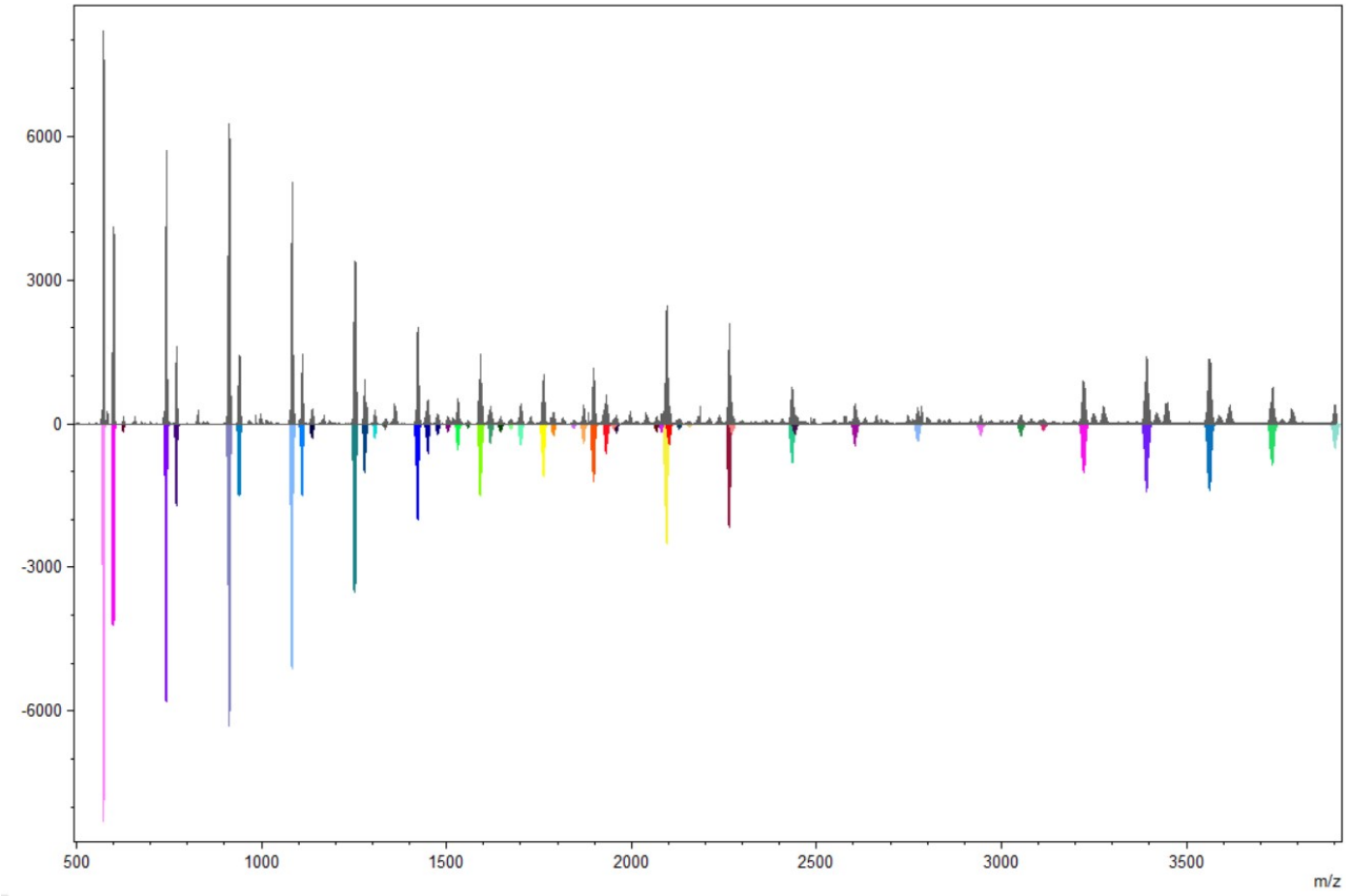

Table S3. Peak assignment for the spectrum of **1** presented in Fig. S11.

anion	m/z exp	m/z calc
$[Ag_3(NO_3)_4]^-$	571.664	571.665
$[Ag_3(C_4H_9S)(NO_3)_3]^-$	598.722	598.723
$[Ag_3(C_4H_9S)_2(NO_3)_2]^-$	625.777	625.778
$[Ag_4(NO_3)_5]^-$	741.556	741.560
$[Ag_4(C_4H_9S)(NO_3)_4]^-$	768.615	768.613
$[Ag_5(NO_3)_6]^-$	911.450	911.451
$[Ag_5(C_4H_9S)(NO_3)_5]^-$	938.501	938.508
$[Ag_6(NO_3)_7]^-$	1081.348	1081.343
$[Ag_6(C_4H_9S)(NO_3)_6]^-$	1108.396	1108.400
$[Ag_6(C_4H_9S)_2(NO_3)_5]^-$	1135.458	1135.454
$[Ag_7(NO_3)_8]^-$	1251.237	1251.236
$[Ag_7(C_4H_9S)(NO_3)_7]^-$	1278.295	1278.293
$[Ag_7(C_4H_9S)_2(NO_3)_6]^-$	1305.343	1305.349
$[Ag_7(C_4H_9S)_3(NO_3)_5]^-$	1332.402	1332.403
$[Ag_8(NO_3)_9]^-$	1421.127	1421.131
$[Ag_8(C_4H_9S)(NO_3)_8]^-$	1448.179	1448.185
$[Ag_8(C_4H_9S)_2(NO_3)_7]^-$	1475.236	1475.239
$[Ag_8(C_4H_9S)_3(NO_3)_6]^-$	1502.295	1502.294
$[Ag_8(C_4H_9S)_4(NO_3)_5]^-$	1529.341	1529.349
$[Ag_8(C_4H_9S)_5(NO_3)_4]^-$	1556.411	1556.403
$[Ag_9(NO_3)_{10}]^-$	1591.027	1591.022
$[Ag_9(C_4H_9S)(NO_3)_9]^-$	1618.083	1618.079
$[Ag_9(C_4H_9S)_2(NO_3)_8]^-$	1645.133	1645.134
$[Ag_9(C_4H_9S)_3(NO_3)_7]^-$	1672.191	1672.188
$[Ag_9(C_4H_9S)_4(NO_3)_6]^-$	1699.250	1699.244
$[Ag_{10}(NO_3)_{11}]^-$	1760.913	1760.916
$[Ag_{10}(C_4H_9S)(NO_3)_{10}]^-$	1787.977	1787.971
$[Ag_{10}(C_4H_9S)_3(NO_3)_8]^-$	1842.082	1842.079
$[Ag_{10}(C_4H_9S)_4(NO_3)_7]^-$	1869.130	1869.134
$[Ag_{20}(C_4H_9S)_{10}(NO_3)_{12}]^{2-}$	1896.687	1896.690
$[Ag_{11}(NO_3)_{12}]^-$	1930.805	1930.808
$[Ag_{11}(C_4H_9S)(NO_3)_{11}]^-$	1957.862	1957.864
$[Ag_{11}(C_4H_9S)_5(NO_3)_7]^-$	2066.091	2066.084
$[Ag_{22}(C_4H_9S)_{11}(NO_3)_{13}]^{2-}$	2080.111	2080.110
$[Ag_{11}(C_4H_9S)_6(NO_3)_6]^-$	2094.134	2094.136
$[Ag_{12}(NO_3)_{13}]^-$	2100.697	2100.702
$[Ag_{12}(C_4H_9S)(NO_3)_{12}]^-$	2127.763	2127.756
$[Ag_{12}(C_4H_9S)_2(NO_3)_{11}]^-$	2154.802	2154.810
$[Ag_{24}(C_4H_9S)_{12}(NO_3)_{14}]^{2-}$	2263.526	2263.529
$[Ag_{13}(NO_3)_{14}]^-$	2270.597	2270.593
$[Ag_{13}(C_4H_9S)_6(NO_3)_8]^-$	2433.912	2433.921
$[Ag_{14}(NO_3)_{15}]^-$	2440.483	2440.487
$[Ag_{14}(C_4H_9S)_6(NO_3)_9]^-$	2602.808	2602.814
$[Ag_{15}(C_4H_9S)_6(NO_3)_{10}]^-$	2772.716	2772.709
$[Ag_{16}(C_4H_9S)_6(NO_3)_{11}]^-$	2942.606	2942.600
$[Ag_{16}(C_4H_9S)_{10}(NO_3)_7]^-$	3051.810	3051.821
$[Ag_{17}(C_4H_9S)_6(NO_3)_{12}]^-$	3112.500	3112.495

$[Ag_{17}(C_4H_9S)_{10}(NO_3)_8]^-$	3221.720	3221.710
$[Ag_{18}(C_4H_9S)_{10}(NO_3)_9]^-$	3391.609	3391.606
$[Ag_{19}(C_4H_9S)_{10}(NO_3)_{10}]^-$	3561.504	3561.495
$[Ag_{20}(C_4H_9S)_{10}(NO_3)_{11}]^-$	3731.389	3731.392
$[Ag_{21}(C_4H_9S)_{10}(NO_3)_{12}]^-$	3901.286	3901.282

Fig. S12. The comparison of observed and calculated isotopic patterns for the spectrum of **1** presented in Fig. S11.

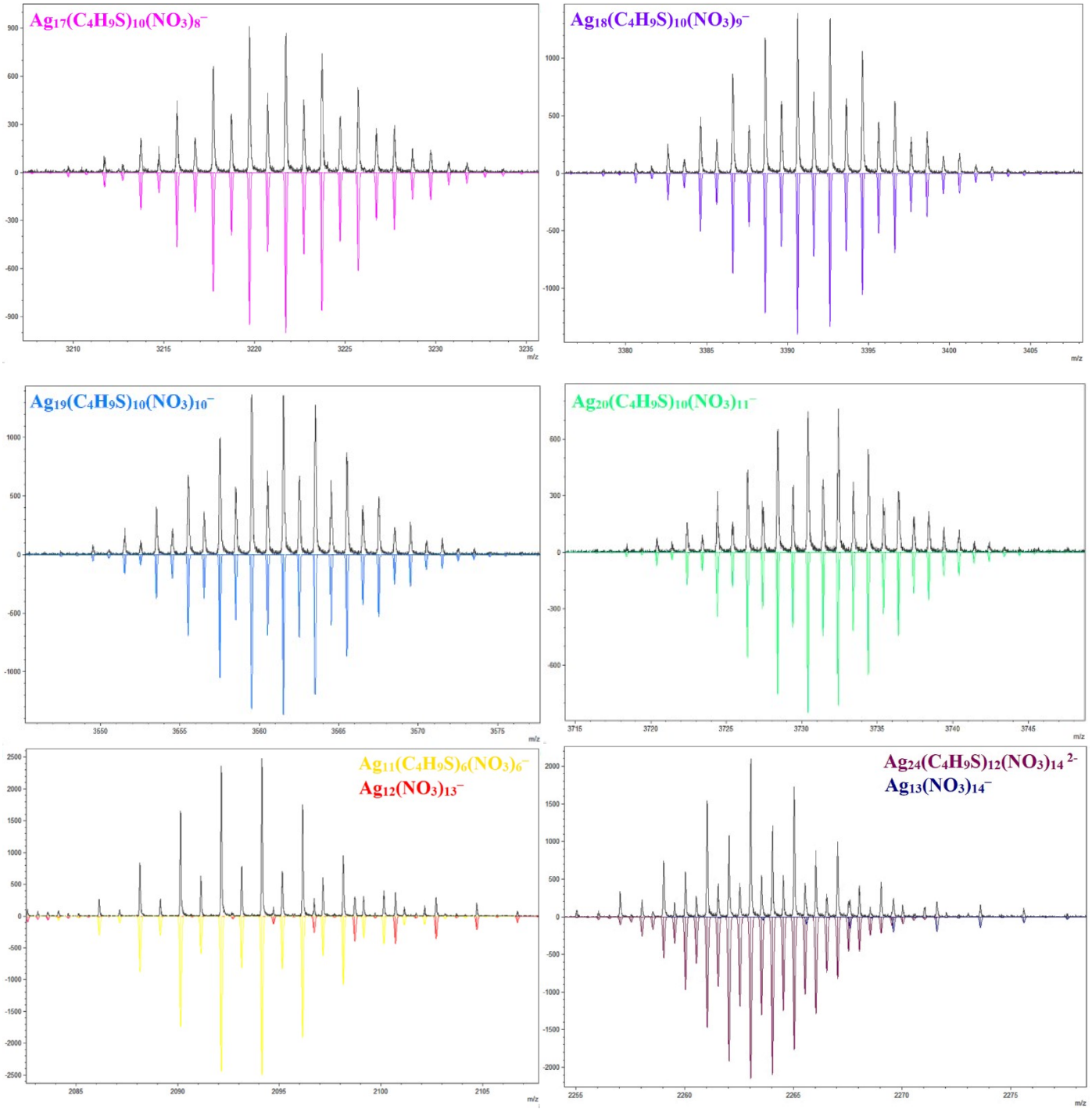

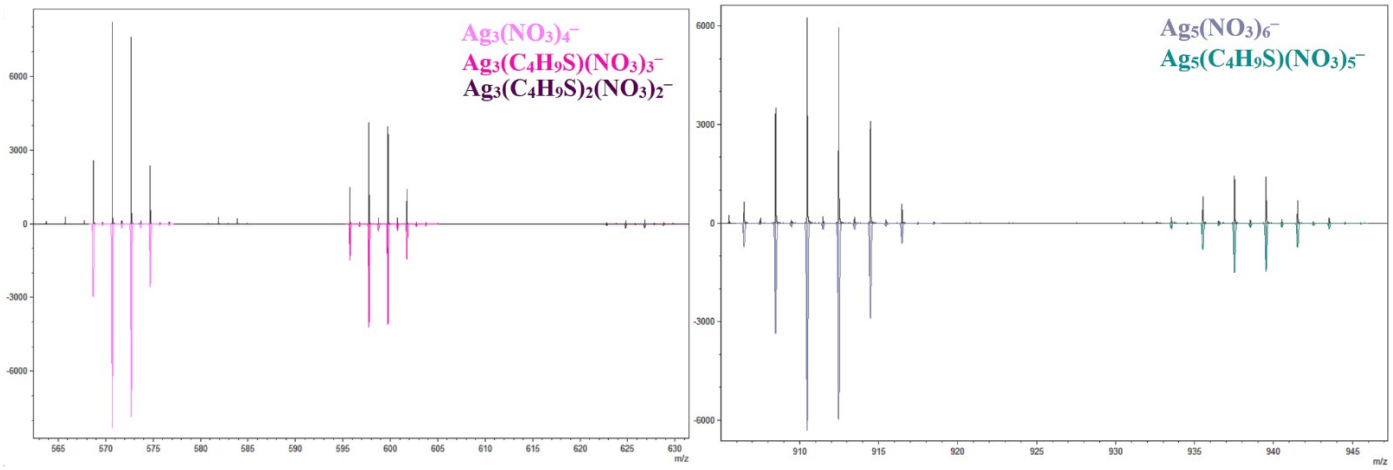
$Ag_3(NO_3)_4^-$
$Ag_3(C_4H_9S)(NO_3)_3^-$
$Ag_3(C_4H_9S)_2(NO_3)_2^-$
$Ag_5(NO_3)_6^-$
$Ag_5(C_4H_9S)(NO_3)_5^-$
m/z
m/z

Fig. S13. Full HR-ESI-MS(+) spectrum of **1** in CH_3CN solution.

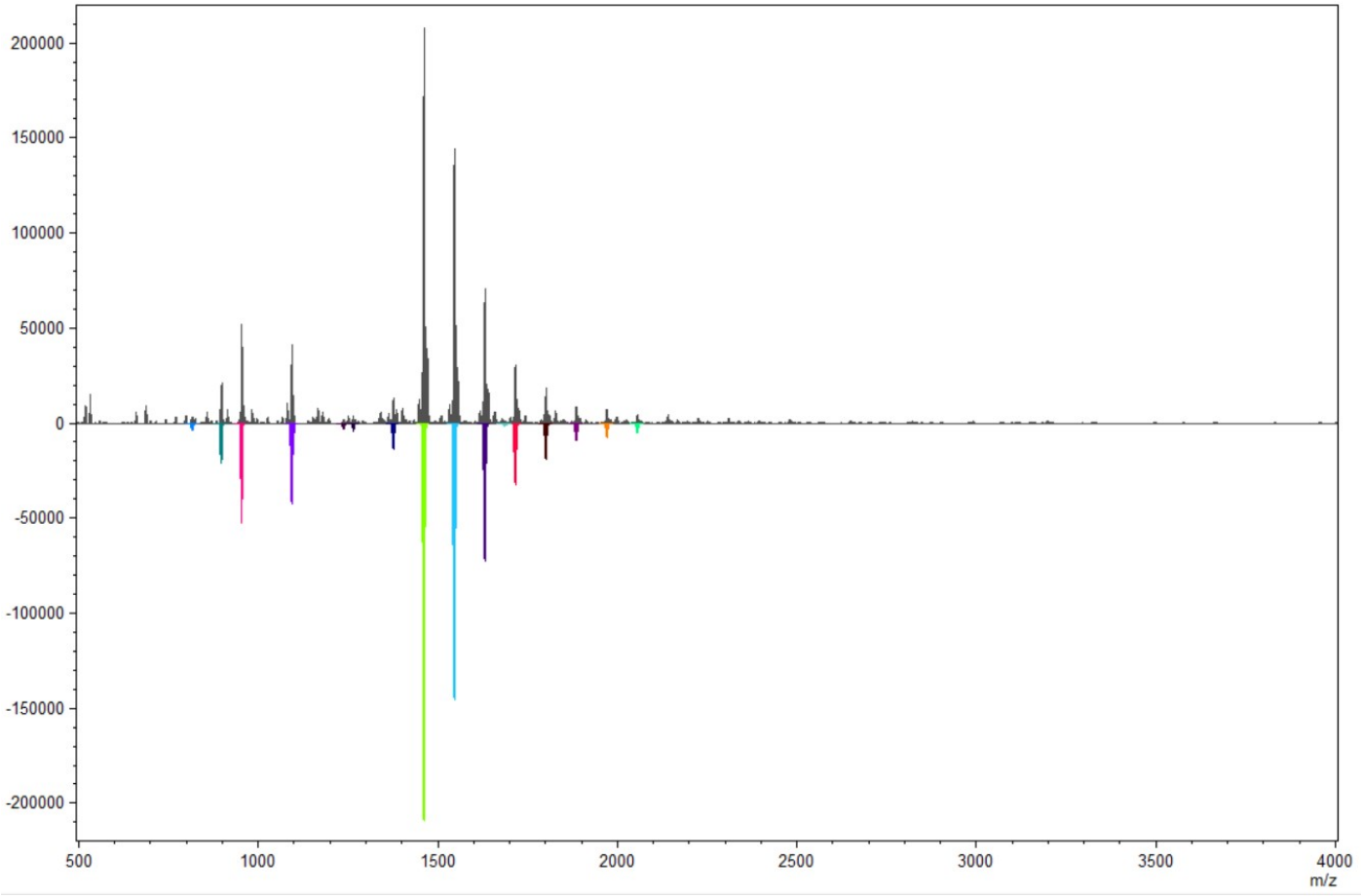

Table S4. Peak assignment for the spectrum of **1** presented in Fig. S13.

cation	m/z exp	m/z calc
$[Ag_5(C_4H_9S)(NO_3)_3]^+$	814.531	814.532
$[Ag_{10}(C_4H_9S)_8]^{2+}$	896.192	896.195
$[Ag_{16}(C_4H_9S)_{12}(NO_3)]^{3+}$	952.661	952.659
$[Ag_6(C_4H_9S)_5]^+$	1092.638	1092.641
$[Ag_7(C_4H_9S)_4(NO_3)_2]^+$	1235.475	1235.482
$[Ag_{14}(C_4H_9S)_{10}(NO_3)_2]^{2+}$	1264.035	1264.043
$[Ag_{15}(C_4H_9S)_{12}(NO_3)]^{2+}$	1375.036	1375.035
$[Ag_{16}(C_4H_9S)_{12}(NO_3)_2]^{2+}$	1459.983	1459.982
$[Ag_{17}(C_4H_9S)_{12}(NO_3)_3]^{2+}$	1544.926	1544.928
$[Ag_{18}(C_4H_9S)_{12}(NO_3)_4]^{2+}$	1629.873	1629.875
$[Ag_{19}(C_4H_9S)_{12}(NO_3)_5]^{2+}$	1714.819	1714.820
$[Ag_{20}(C_4H_9S)_{12}(NO_3)_6]^{2+}$	1799.769	1799.768
$[Ag_{21}(C_4H_9S)_{12}(NO_3)_7]^{2+}$	1884.715	1884.713
$[Ag_{22}(C_4H_9S)_{12}(NO_3)_8]^{2+}$	1969.665	1969.660
$[Ag_{23}(C_4H_9S)_{12}(NO_3)_9]^{2+}$	2054.604	2054.606

Fig. S14. The comparison of observed and calculated isotopic patterns for the spectrum of **1** presented in Fig. S13.

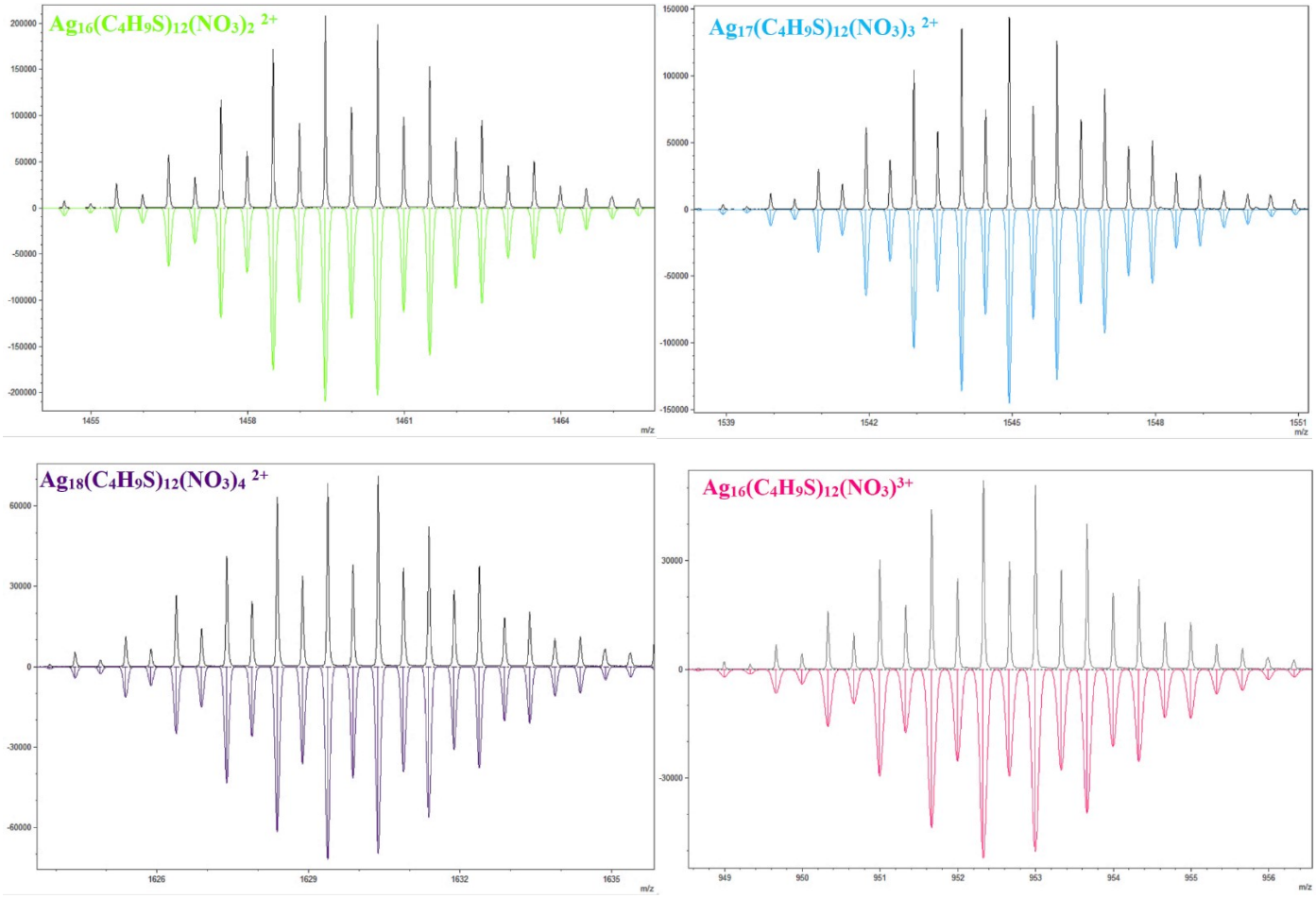

Fig. S15. Full HR-ESI-MS(+) spectrum of **1** in CH_3CN solution after some period of time.

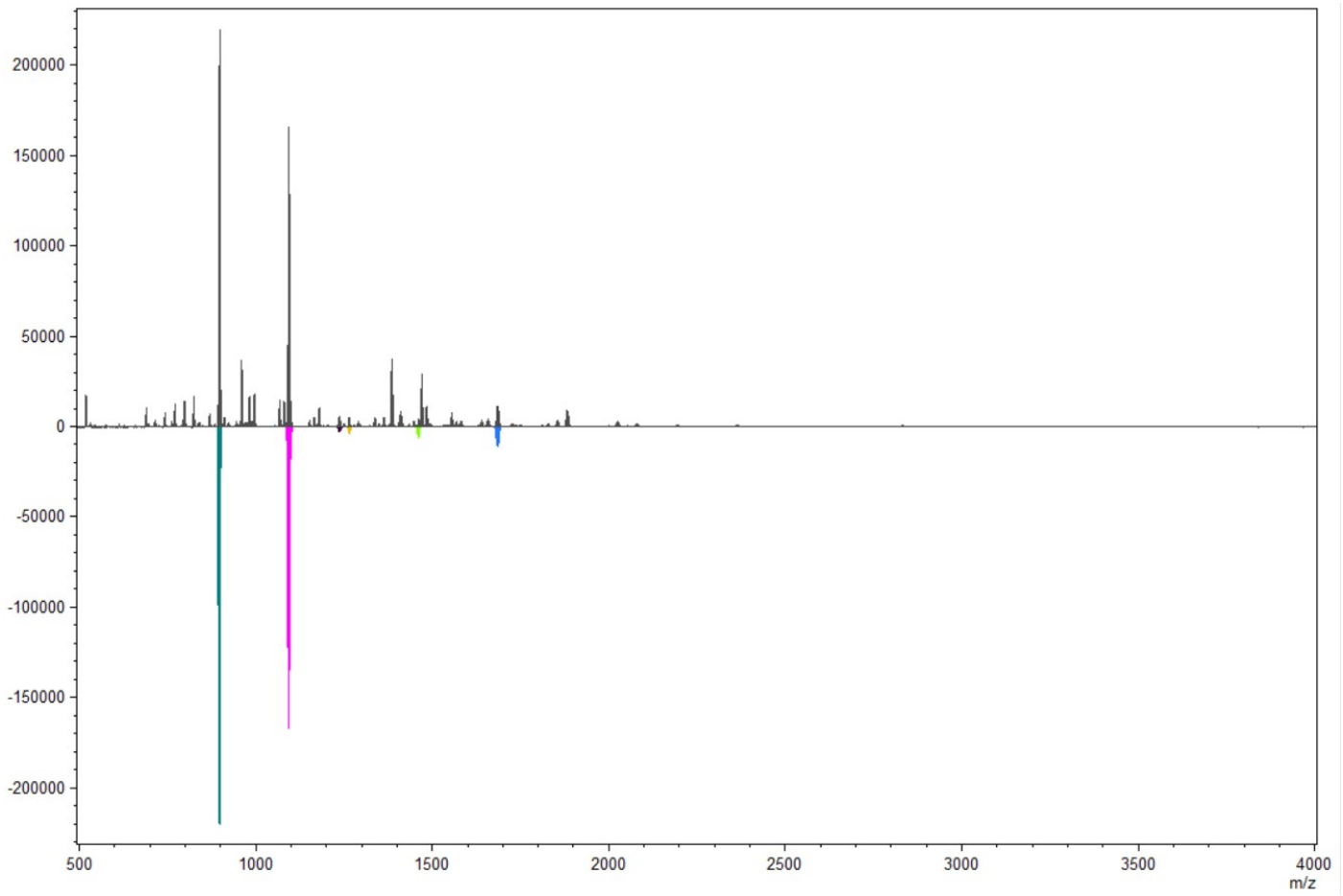

Table S5. Peak assignment for the spectrum of **1** presented in Fig. S15.

cation	m/z exp	m/z calc
$[Ag_{10}(C_4H_9S)_8]^{2+}$	896.197	896.195
$[Ag_6(C_4H_9S)_5]^{+}$	1092.643	1092.641
$[Ag_7(C_4H_9S)_4(NO_3)_2]^{+}$	1253.480	1235.482
$[Ag_{14}(C_4H_9S)_{10}(NO_3)_2]^{2+}$	1264.035	1264.043
$[Ag_{16}(C_4H_9S)_{12}(NO_3)_2]^{2+}$	1459.987	1459.982
$[Ag_9(C_4H_9S)_8]^{+}$	1684.485	1684.483

Fig. S16. The comparison of observed and calculated isotopic patterns for the spectrum of **1** presented in Fig. S15.

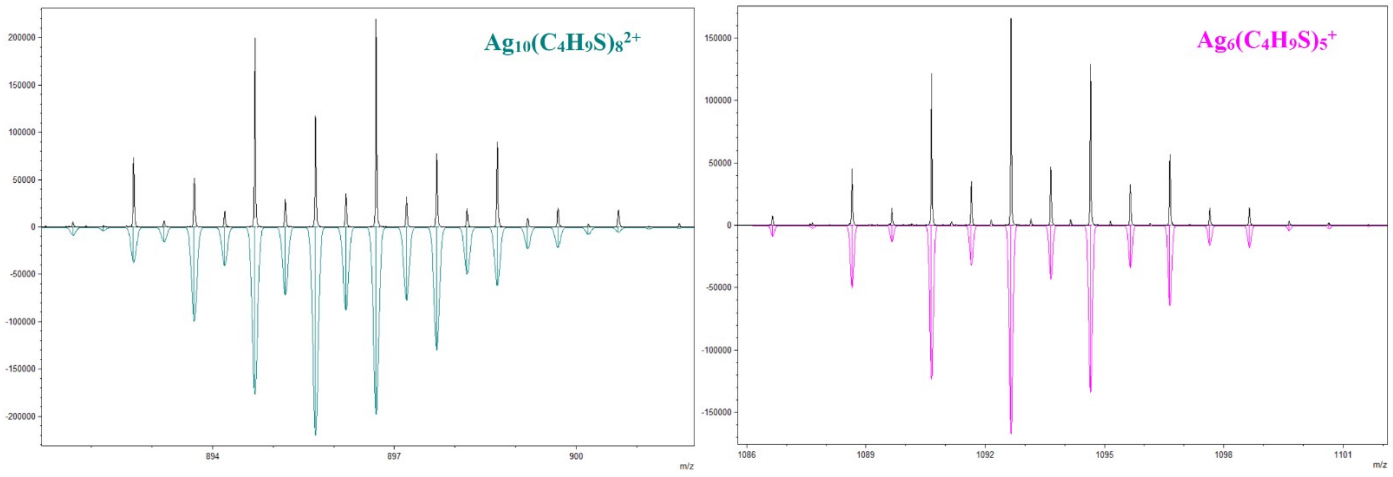

Fig. S17. Full HR-ESI-MS(-) spectrum of **2** in CH_3CN solution.

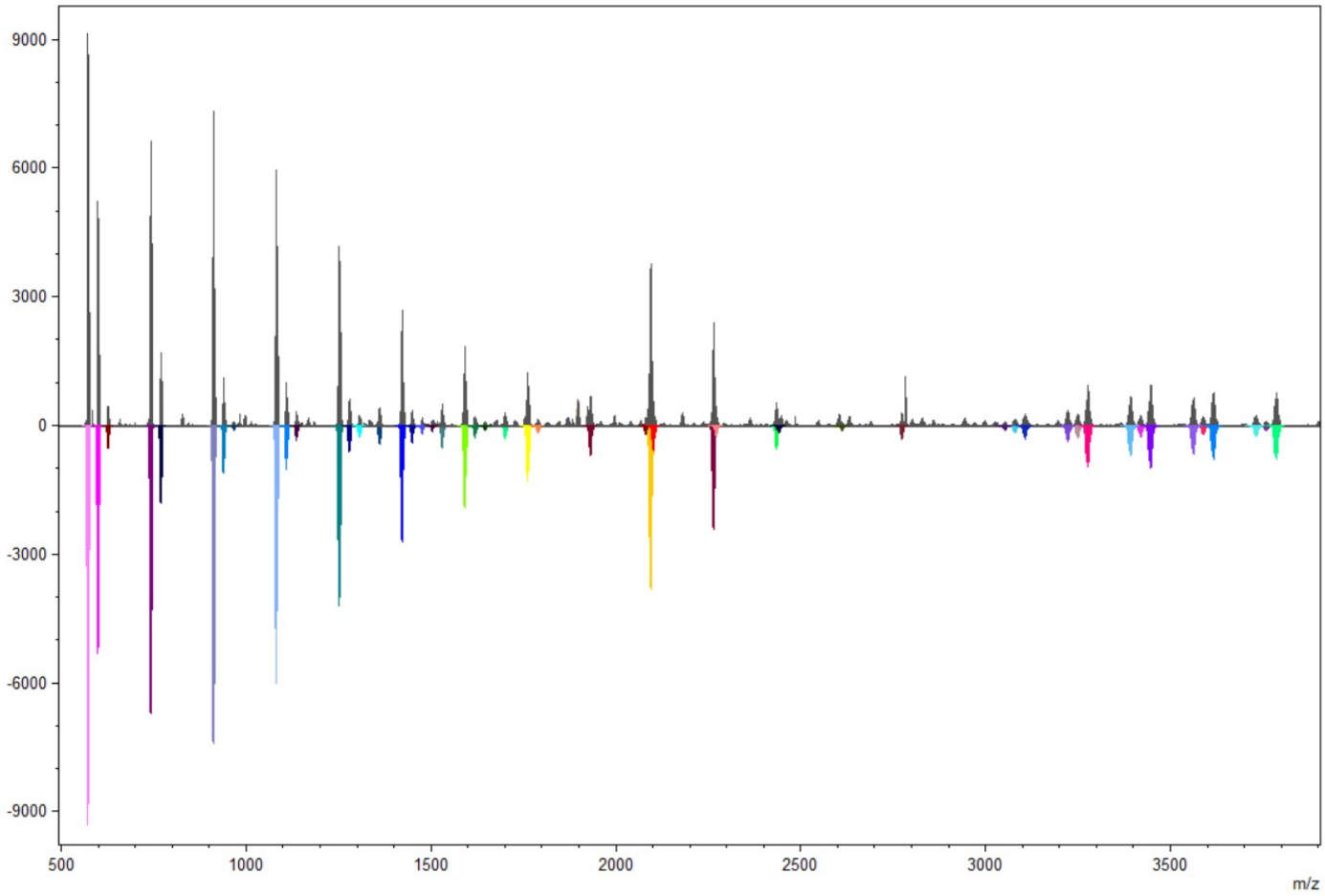

Table S6. Peak assignment for the spectrum of **2** presented in Fig. S17.

anion	m/z exp	m/z calc
$[Ag_3(NO_3)_4]^-$	571.662	571.666
$[Ag_3(C_4H_9S)(NO_3)_3]^-$	598.722	598.723
$[Ag_3(C_4H_9S)_2(NO_3)_2]^-$	625.784	625.778
$[Ag_4(NO_3)_5]^-$	741.559	741.560
$[Ag_4(C_4H_9S)(NO_3)_4]^-$	768.611	768.614
$[Ag_5(NO_3)_6]^-$	911.455	911.451
$[Ag_5(C_4H_9S)(NO_3)_5]^-$	938.514	938.508
$[Ag_5(C_4H_9S)_2(NO_3)_4]^-$	965.568	965.563
$[Ag_6(NO_3)_7]^-$	1081.341	1081.345
$[Ag_6(C_4H_9S)(NO_3)_6]^-$	1108.400	1108.400
$[Ag_6(C_4H_9S)_2(NO_3)_5]^-$	1135.452	1135.454
$[Ag_7(NO_3)_8]^-$	1251.236	1251.237
$[Ag_7(C_4H_9S)(NO_3)_7]^-$	1278.294	1278.294
$[Ag_7(C_4H_9S)_2(NO_3)_6]^-$	1305.352	1305.349
$[Ag_7(C_4H_9S)_4(NO_3)_4]^-$	1359.461	1359.458
$[Ag_8(NO_3)_9]^-$	1421.126	1421.131
$[Ag_8(C_4H_9S)(NO_3)_8]^-$	1448.176	1448.185
$[Ag_8(C_4H_9S)_2(NO_3)_7]^-$	1475.238	1475.240
$[Ag_8(C_4H_9S)_3(NO_3)_6]^-$	1502.289	1502.294
$[Ag_8(C_4H_9S)_4(NO_3)_5]^-$	1529.351	1529.345
$[Ag_9(NO_3)_{10}]^-$	1591.026	1591.022
$[Ag_9(C_4H_9S)(NO_3)_9]^-$	1618.071	1618.079
$[Ag_9(C_4H_9S)_2(NO_3)_8]^-$	1645.133	1645.134
$[Ag_9(C_4H_9S)_4(NO_3)_6]^-$	1699.243	1699.244
$[Ag_{10}(NO_3)_{11}]^-$	1760.912	1760.916
$[Ag_{10}(C_4H_9S)(NO_3)_{10}]^-$	1787.971	1787.971
$[Ag_{10}(C_4H_9S)_4(NO_3)_7]^-$	1869.129	1869.134
$[Ag_{20}(C_4H_9S)_{10}(NO_3)_{12}]^{2-}$	1896.686	1896.690
$[Ag_{11}(NO_3)_{12}]^-$	1930.816	1930.808
$[Ag_{22}(C_4H_9S)_{11}(NO_3)_{13}]^{2-}$	2080.097	2080.110
$[Ag_{11}(C_4H_9S)_6(NO_3)_6]^-$	2094.133	2094.136
$[Ag_{12}(NO_3)_{13}]^-$	2100.695	2100.701
$[Ag_{24}(C_4H_9S)_{12}(NO_3)_{14}]^{2-}$	2263.538	2263.530
$[Ag_{13}(NO_3)_{14}]^-$	2270.588	2270.593
$[Ag_{26}(C_4H_9S)_{12}(NO_3)_{16}]^{2-}$	2433.421	2433.423
$[Ag_{14}(NO_3)_{15}]^-$	2440.481	2440.487
$[Ag_{15}(NO_3)_{16}]^-$	2610.381	2610.379
$[Ag_{16}(C_4H_9S)_{10}(NO_3)_7]^-$	3051.824	3051.820
$[Ag_{16}(C_4H_9S)_{11}(NO_3)_6]^-$	3078.880	3078.875
$[Ag_{16}(C_4H_9S)_{12}(NO_3)_5]^-$	3105.922	3105.930
$[Ag_{17}(C_4H_9S)_{10}(NO_3)_8]^-$	3221.719	3221.711
$[Ag_{17}(C_4H_9S)_{11}(NO_3)_7]^-$	3248.764	3248.765
$[Ag_{17}(C_4H_9S)_{12}(NO_3)_6]^-$	3275.819	3275.820
$[Ag_{18}(C_4H_9S)_{10}(NO_3)_9]^-$	3391.607	3391.606
$[Ag_{18}(C_4H_9S)_{11}(NO_3)_8]^-$	3418.657	3418.661
$[Ag_{18}(C_4H_9S)_{12}(NO_3)_7]^-$	3445.718	3445.715
$[Ag_{19}(C_4H_9S)_{10}(NO_3)_{10}]^-$	3561.499	3561.496
$[Ag_{19}(C_4H_9S)_{11}(NO_3)_9]^-$	3588.546	3588.551
$[Ag_{19}(C_4H_9S)_{12}(NO_3)_8]^-$	3615.603	3615.606

$[Ag_{20}(C_4H_9S)_{10}(NO_3)_{11}]^-$	3731.397	3731.392
$[Ag_{20}(C_4H_9S)_{11}(NO_3)_{10}]^-$	3758.444	3758.446
$[Ag_{20}(C_4H_9S)_{12}(NO_3)_9]^-$	3785.511	3785.500

Fig. S18. The comparison of observed and calculated isotopic patterns for the spectrum of **2** presented in Fig. S17.

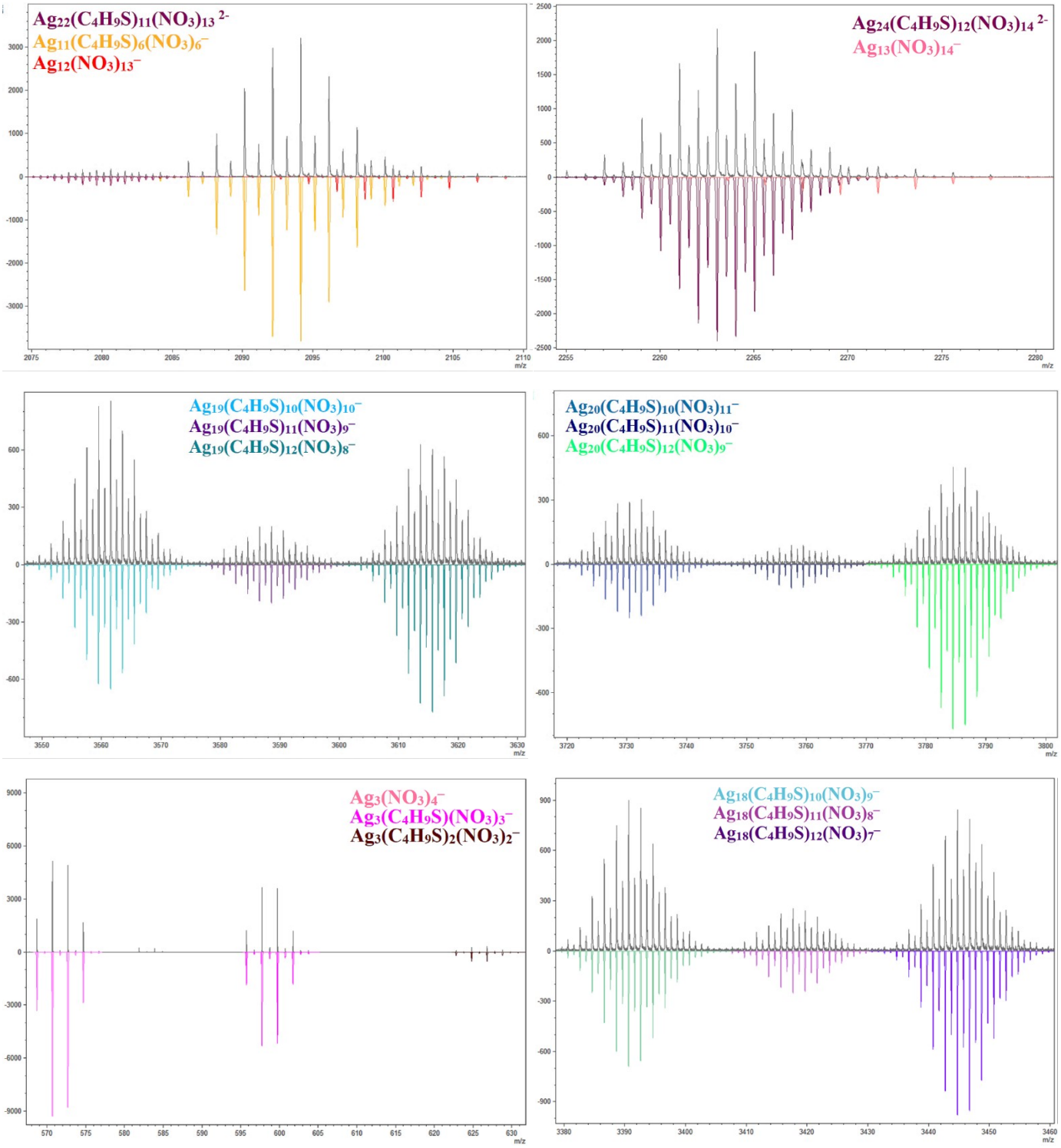

Fig. S19. Full HR-ESI-MS(+) spectrum of **2** in CH_3CN solution.

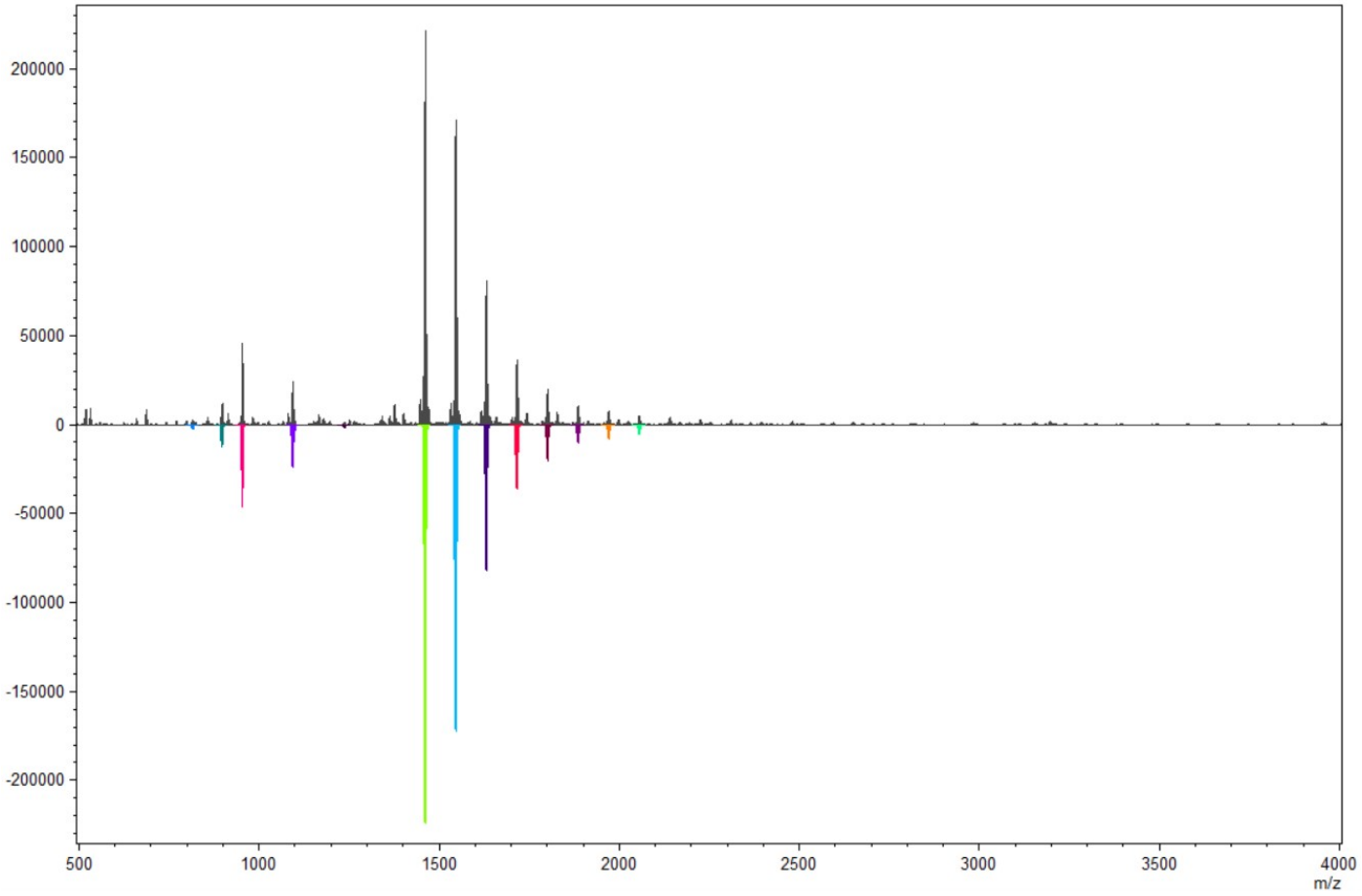

Table S7. Peak assignment for the spectrum of **2** presented in Fig. S19.

cation	m/z exp	m/z calc
$[Ag_5(C_4H_9S)(NO_3)_3]^+$	814.527	814.532
$[Ag_{10}(C_4H_9S)_8]^{2+}$	896.192	896.195
$[Ag_{16}(C_4H_9S)_{12}(NO_3)]^{3+}$	952.660	952.659
$[Ag_6(C_4H_9S)_5]^+$	1092.638	1092.641
$[Ag_{14}(C_4H_9S)_{10}(NO_3)_2]^{2+}$	1235.986	1235.980
$[Ag_{16}(C_4H_9S)_{12}(NO_3)_2]^{2+}$	1459.983	1459.982
$[Ag_{17}(C_4H_9S)_{12}(NO_3)_3]^{2+}$	1544.931	1544.928
$[Ag_{18}(C_4H_9S)_{12}(NO_3)_4]^{2+}$	1629.873	1629.875
$[Ag_{19}(C_4H_9S)_{12}(NO_3)_5]^{2+}$	1714.819	1714.820
$[Ag_{20}(C_4H_9S)_{12}(NO_3)_6]^{2+}$	1799.769	1799.768
$[Ag_{21}(C_4H_9S)_{12}(NO_3)_7]^{2+}$	1884.715	1884.713
$[Ag_{22}(C_4H_9S)_{12}(NO_3)_8]^{2+}$	1969.658	1969.661
$[Ag_{23}(C_4H_9S)_{12}(NO_3)_9]^{2+}$	2054.610	2054.606

Fig. S20. The comparison of observed and calculated isotopic patterns for the spectrum of **2** presented in Fig. S19.

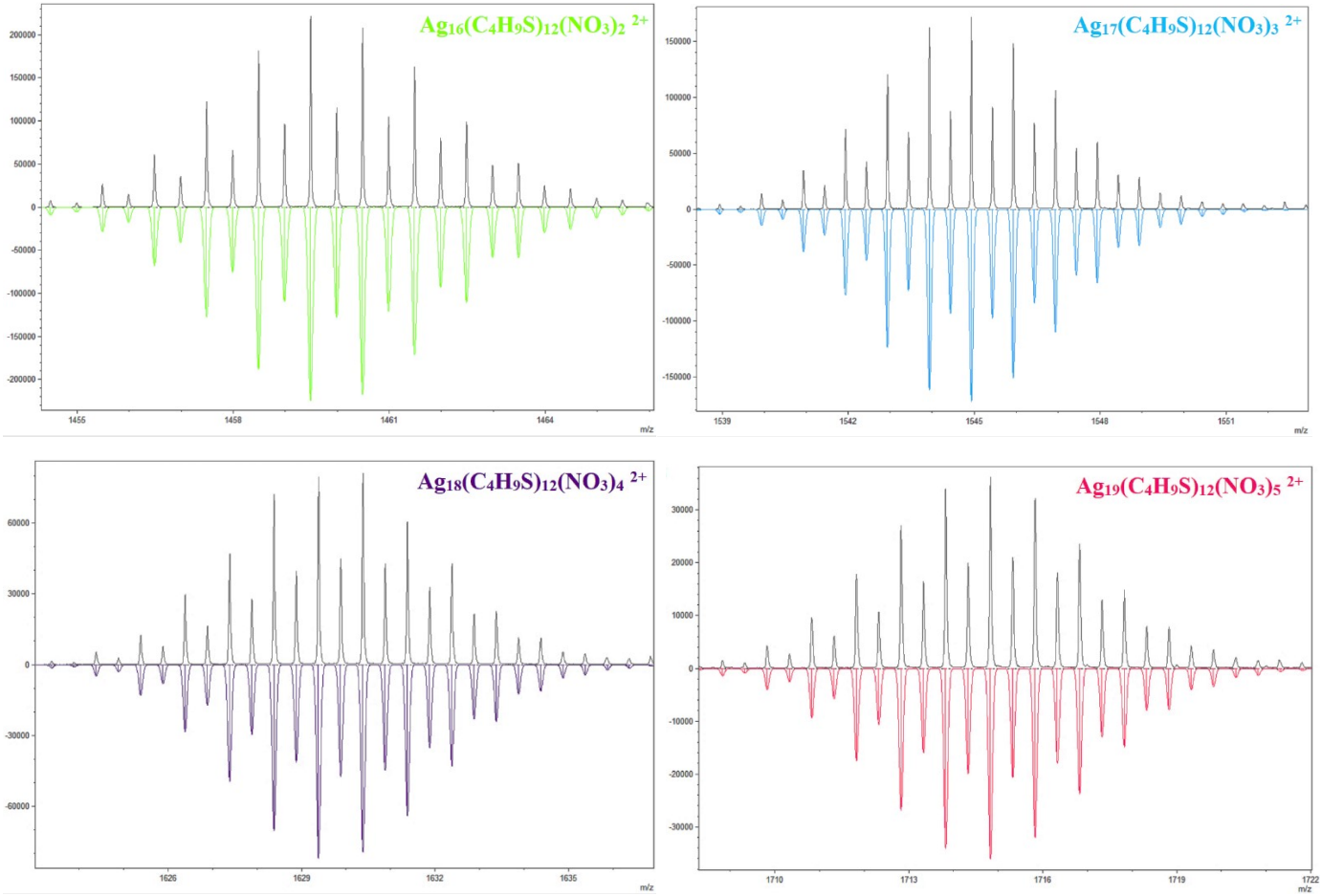

Fig. S21. Full HR-ESI-MS(+) spectrum of **2** in CH_3CN solution after some period of time.

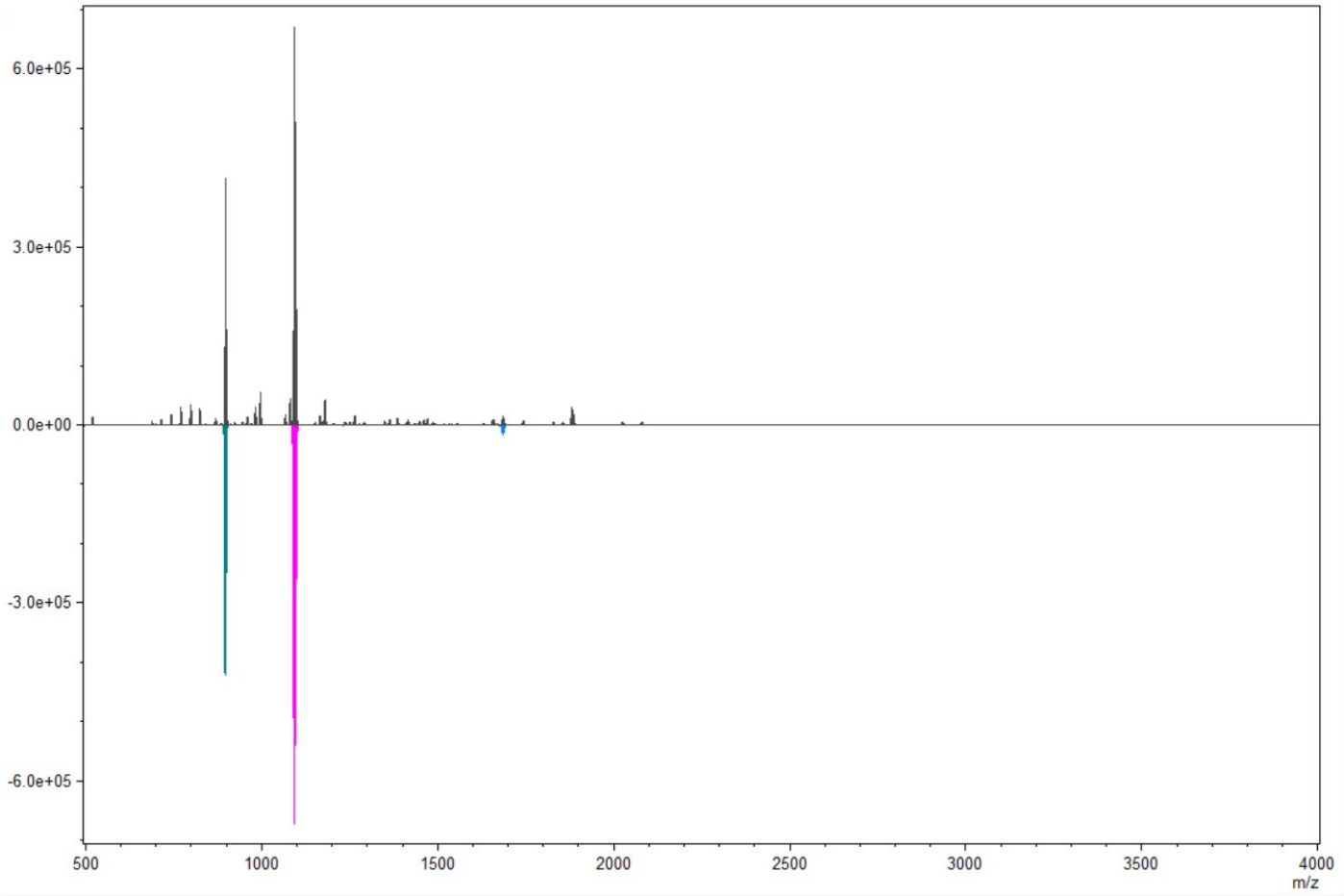

Table S8. Peak assignment for the spectrum of **2** presented in Fig. S21.

cation	m/z exp	m/z calc
$[Ag_{10}(C_4H_9S)_8]^{2+}$	896.197	896.195
$[Ag_6(C_4H_9S)_5]^{+}$	1092.643	1092.641
$[Ag_9(C_4H_9S)_8]^{+}$	1684.485	1684.483

Fig. S22. The comparison of observed and calculated isotopic patterns for the spectrum of **2** presented in Fig. S21.

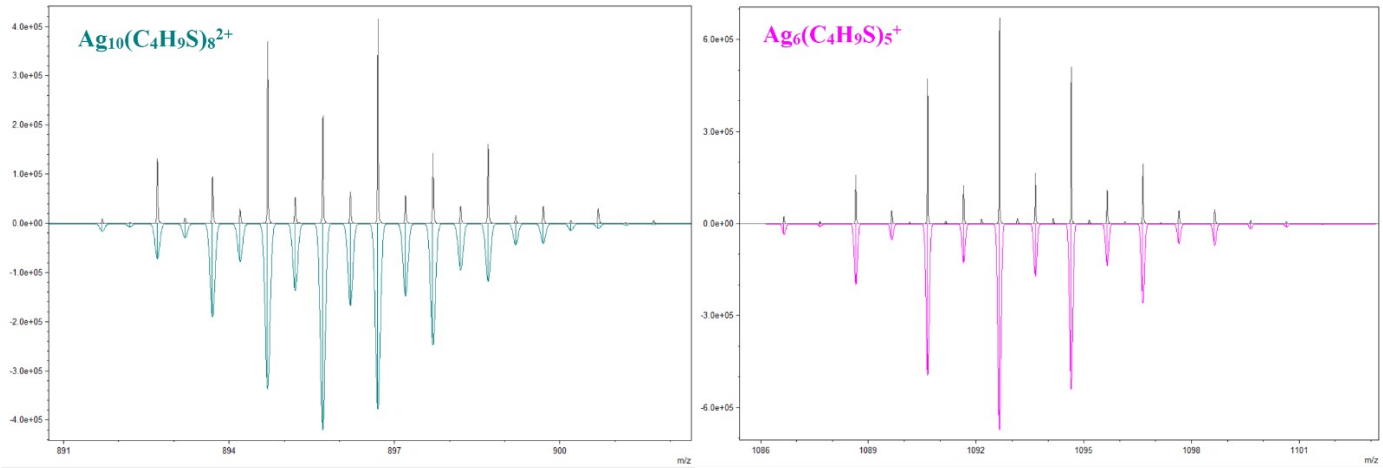

Fig. S23. Full HR-ESI-MS(-) spectrum of **3** in CH_3CN solution.

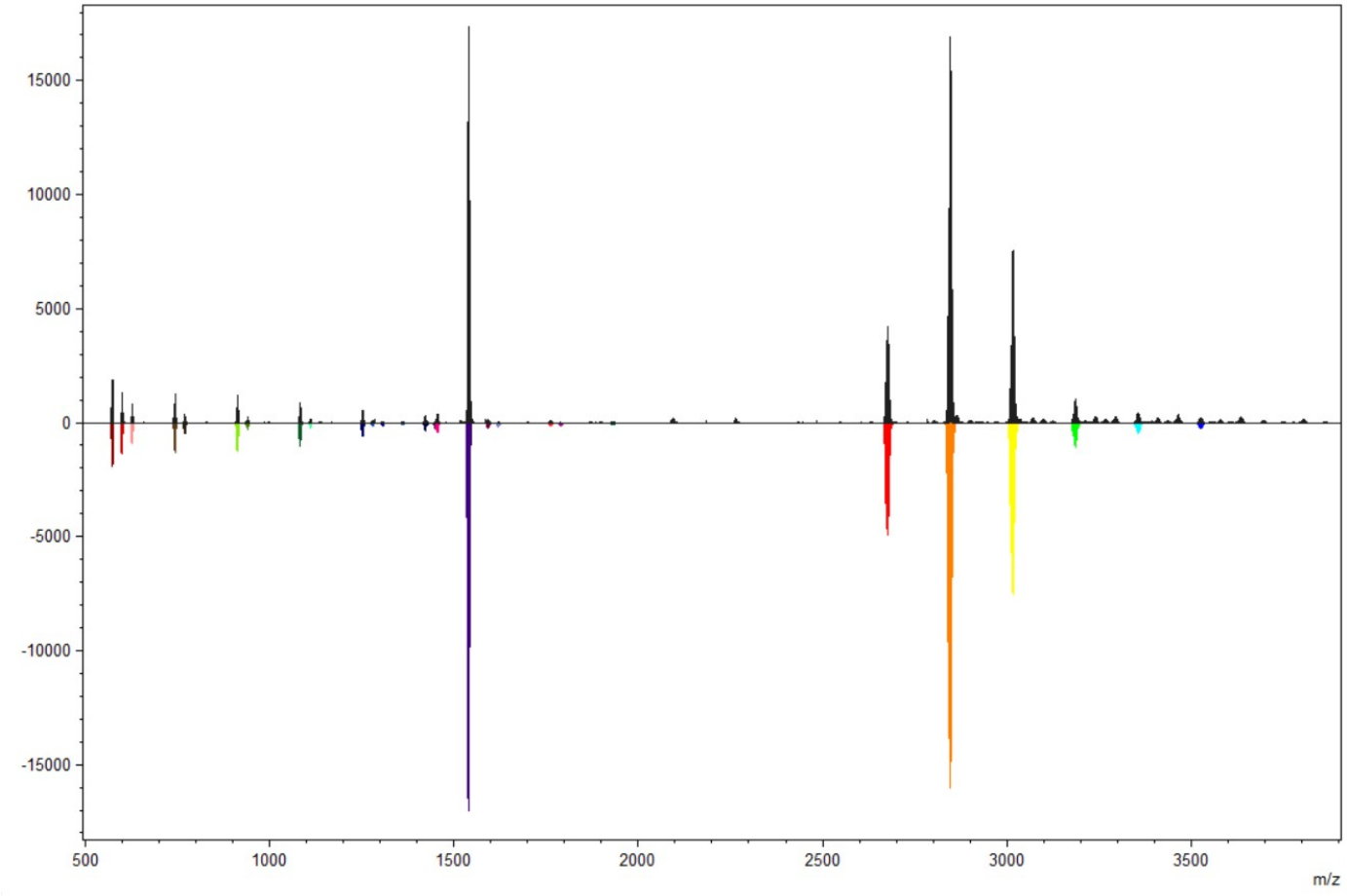

Table S9. Peak assignment for the spectrum of **3** presented in Fig. S23.

anion	m/z exp	m/z calc
$[Ag_3(NO_3)_4]^-$	571.662	571.664
$[Ag_3(C_4H_9S)(NO_3)_3]^-$	598.721	598.722
$[Ag_3(C_4H_9S)_2(NO_3)_2]^-$	625.777	625.778
$[Ag_4(NO_3)_5]^-$	741.558	741.559
$[Ag_4(C_4H_9S)(NO_3)_4]^-$	768.612	768.614
$[Ag_5(NO_3)_6]^-$	911.448	911.451
$[Ag_5(C_4H_9S)(NO_3)_5]^-$	938.502	938.508
$[Ag_6(NO_3)_7]^-$	1081.342	1081.345
$[Ag_6(C_4H_9S)(NO_3)_6]^-$	1108.402	1108.399
$[Ag_7(NO_3)_8]^-$	1251.242	1251.237
$[Ag_7(C_4H_9S)(NO_3)_7]^-$	1278.290	1278.293
$[Ag_7(C_4H_9S)_2(NO_3)_6]^-$	1305.353	1305.348
$[Ag_7(C_4H_9S)_4(NO_3)_4]^-$	1359.467	1359.458
$[Ag_8(NO_3)_9]^-$	1421.127	1421.130
$[Ag_8(C_4H_9S)(NO_3)_8]^-$	1448.177	1448.185
$[Ag_{15}(C_4H_9S)_8(NO_3)_8Br]^{2-}$	1453.866	1453.868
$[Ag_{16}(C_4H_9S)_8(NO_3)_9Br]^{2-}$	1538.809	1538.813
$[Ag_9(NO_3)_{10}]^-$	1591.017	1591.022
$[Ag_9(C_4H_9S)(NO_3)_9]^-$	1618.078	1618.079
$[Ag_{10}(NO_3)_{11}]^-$	1760.920	1760.916
$[Ag_{10}(C_4H_9S)(NO_3)_{10}]^-$	1787.982	1787.971
$[Ag_{11}(NO_3)_{12}]^-$	1930.805	1930.807
$[Ag_{14}(C_4H_9S)_8(NO_3)_6Br]^-$	2675.848	2675.852
$[Ag_{15}(C_4H_9S)_8(NO_3)_7Br]^-$	2845.751	2845.748
$[Ag_{16}(C_4H_9S)_8(NO_3)_8Br]^-$	3015.636	3015.637
$[Ag_{17}(C_4H_9S)_8(NO_3)_9Br]^-$	3185.538	3185.534
$[Ag_{18}(C_4H_9S)_8(NO_3)_{10}Br]^-$	3355.432	3355.423
$[Ag_{19}(C_4H_9S)_8(NO_3)_{11}Br]^-$	3525.327	3525.319

Fig. S24. The comparison of observed and calculated isotopic patterns for the spectrum of **3** presented in Fig. S23.

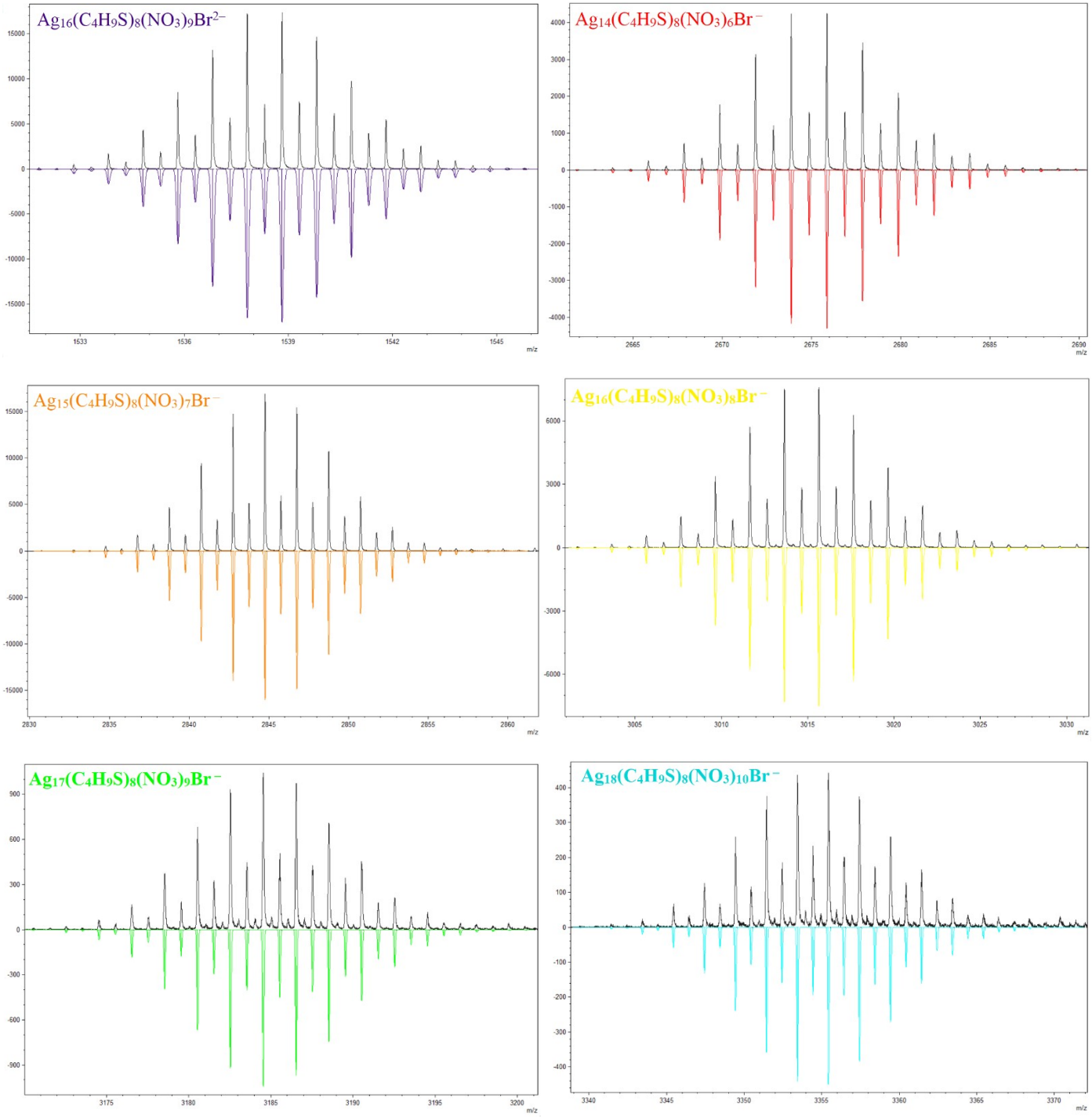

Fig. S25. Full HR-ESI-MS(+) spectrum of **3** in CH_3CN solution.

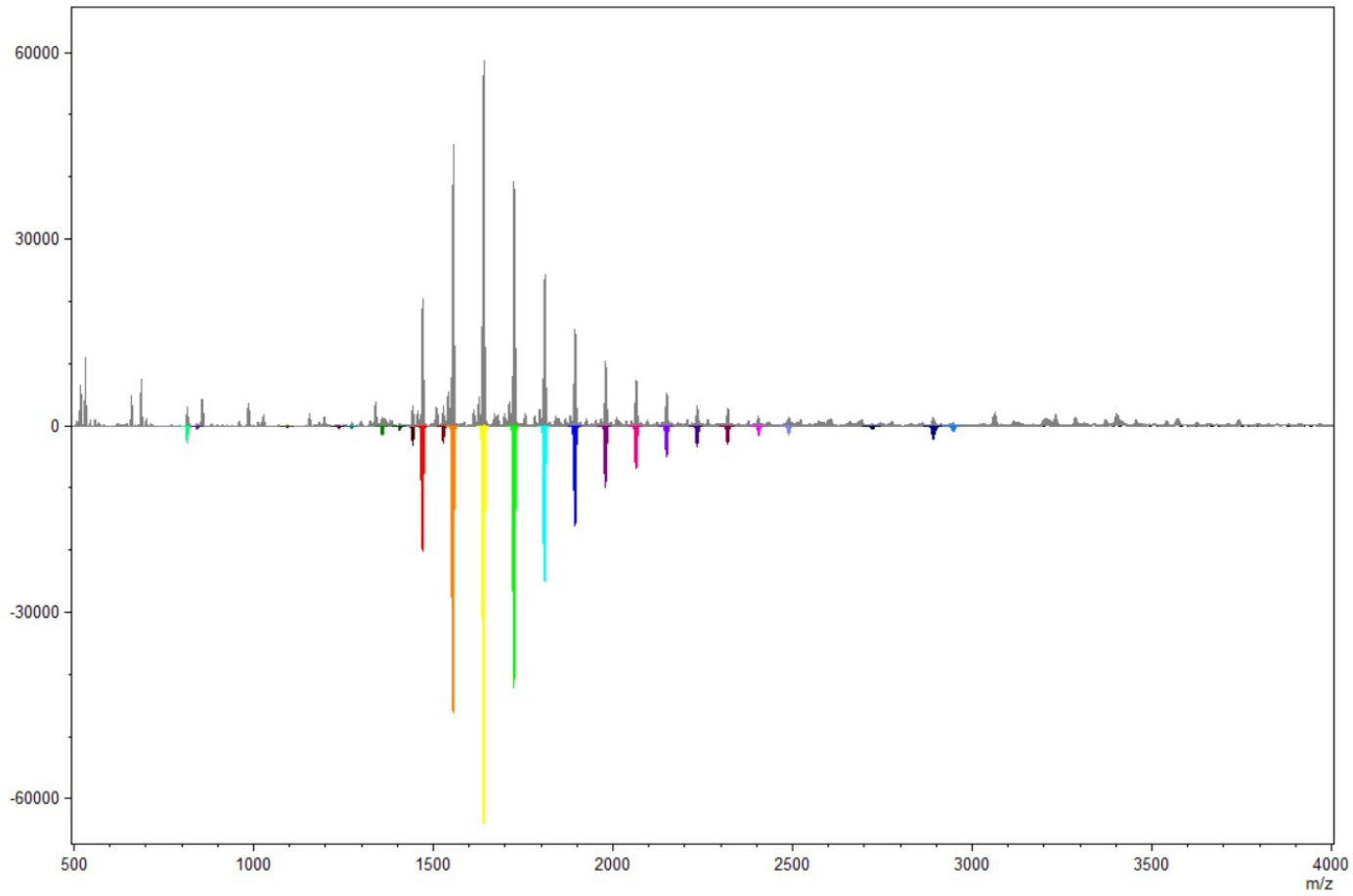

Table S10. Peak assignment for the spectrum of **3** presented in Fig. S25.

cation	m/z exp	m/z calc
$[Ag_5(C_4H_9S)(NO_3)_3]^+$	814.533	814.532
$[Ag_5(C_4H_9S)_2(NO_3)_2]^+$	841.581	841.586
$[Ag_6(C_4H_9S)_5]^+$	1092.638	1092.641
$[Ag_7(C_4H_9S)_4(NO_3)_2]^+$	1235.486	1235.482
$[Ag_{14}(C_4H_9S)_8(NO_3)_4(DMF)]^{2+}$	1272.505	1272.507
$[Ag_{15}(C_4H_9S)_8(NO_3)_5(DMF)]^{2+}$	1357.447	1357.452
$[Ag_{16}(C_4H_9S)_8(NO_3)_6]^{2+}$	1405.882	1405.873
$[Ag_{16}(C_4H_9S)_8(NO_3)_6(DMF)]^{2+}$	1442.399	1442.400
$[Ag_{16}(C_4H_9S)_{12}(NO_3)Br^{2+}$	1468.950	1468.946
$[Ag_{17}(C_4H_9S)_8(NO_3)_7(DMF)]^{2+}$	1527.339	1527.345
$[Ag_{17}(C_4H_9S)_{12}(NO_3)_2Br]^{2+}$	1553.897	1553.894
$[Ag_{18}(C_4H_9S)_{12}(NO_3)_3Br]^{2+}$	1638.838	1638.839
$[Ag_{19}(C_4H_9S)_{12}(NO_3)_4Br]^{2+}$	1723.785	1723.786
$[Ag_{20}(C_4H_9S)_{12}(NO_3)_5Br]^{2+}$	1808.733	1808.731
$[Ag_{21}(C_4H_9S)_{12}(NO_3)_6Br]^{2+}$	1893.681	1893.679
$[Ag_{22}(C_4H_9S)_{12}(NO_3)_7Br]^{2+}$	1978.626	1978.624
$[Ag_{23}(C_4H_9S)_{12}(NO_3)_8Br]^{2+}$	2063.574	2063.572
$[Ag_{24}(C_4H_9S)_{12}(NO_3)_9Br]^{2+}$	2148.516	2148.517
$[Ag_{25}(C_4H_9S)_{12}(NO_3)_{10}Br]^{2+}$	2233.468	2233.464
$[Ag_{26}(C_4H_9S)_{12}(NO_3)_{11}Br]^{2+}$	2318.405	2318.410
$[Ag_{27}(C_4H_9S)_{12}(NO_3)_{12}Br]^{2+}$	2404.357	2404.365
$[Ag_{28}(C_4H_9S)_{12}(NO_3)_{13}Br]^{2+}$	2488.297	2488.302
$[Ag_{15}(C_4H_9S)_8(NO_3)_5Br]^+$	2721.781	2721.772
$[Ag_{16}(C_4H_9S)_8(NO_3)_6Br]^+$	2891.657	2891.661
$[Ag_{16}(C_4H_9S)_8(NO_3)_7Br]^+$	2946.773	2946.787

Fig. S26. The comparison of observed and calculated isotopic patterns for the spectrum of **3** presented in Fig. S25.

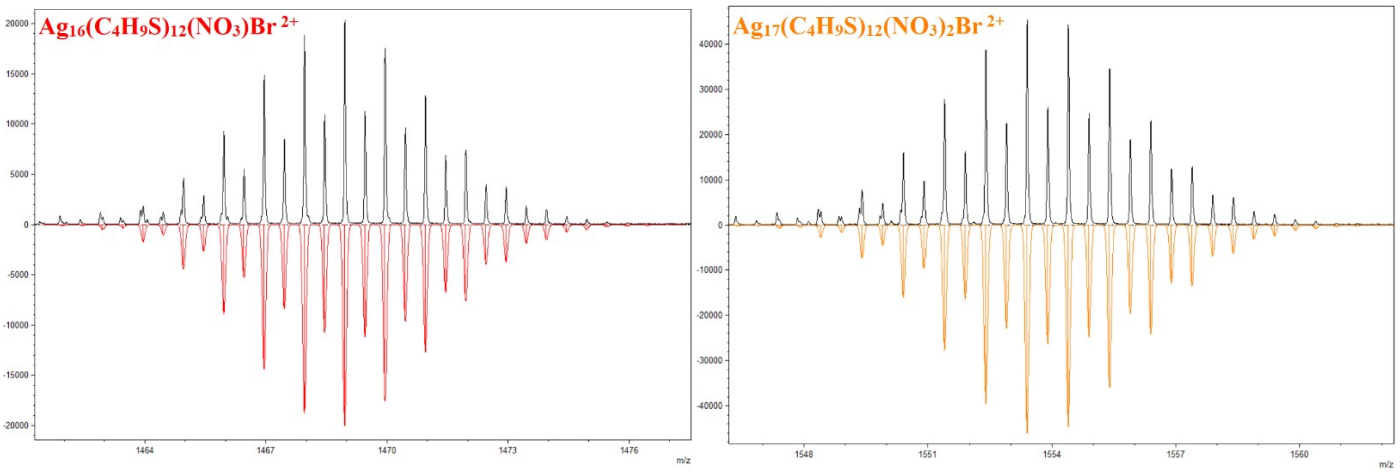

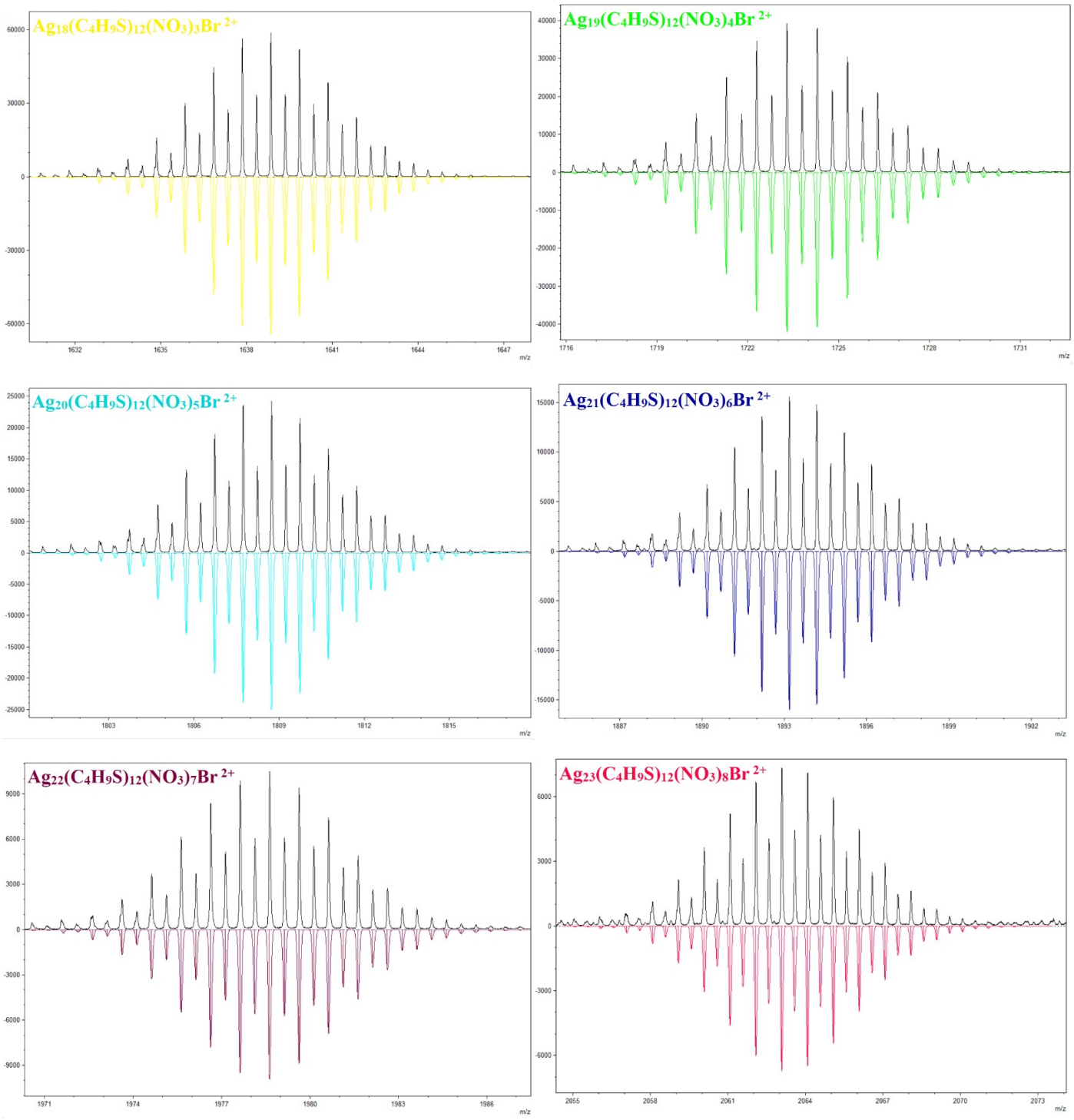
$Ag_{18}(C_4H_9S)_{12}(NO_3)_3Br^{2+}$
$Ag_{19}(C_4H_9S)_{12}(NO_3)_4Br^{2+}$
$Ag_{20}(C_4H_9S)_{12}(NO_3)_5Br^{2+}$
$Ag_{21}(C_4H_9S)_{12}(NO_3)_6Br^{2+}$
$Ag_{22}(C_4H_9S)_{12}(NO_3)_7Br^{2+}$
$Ag_{23}(C_4H_9S)_{12}(NO_3)_8Br^{2+}$
m/z

Fig. S27. Full HR-ESI-MS(+) spectrum of **3** in CH_3CN solution after some period of time.

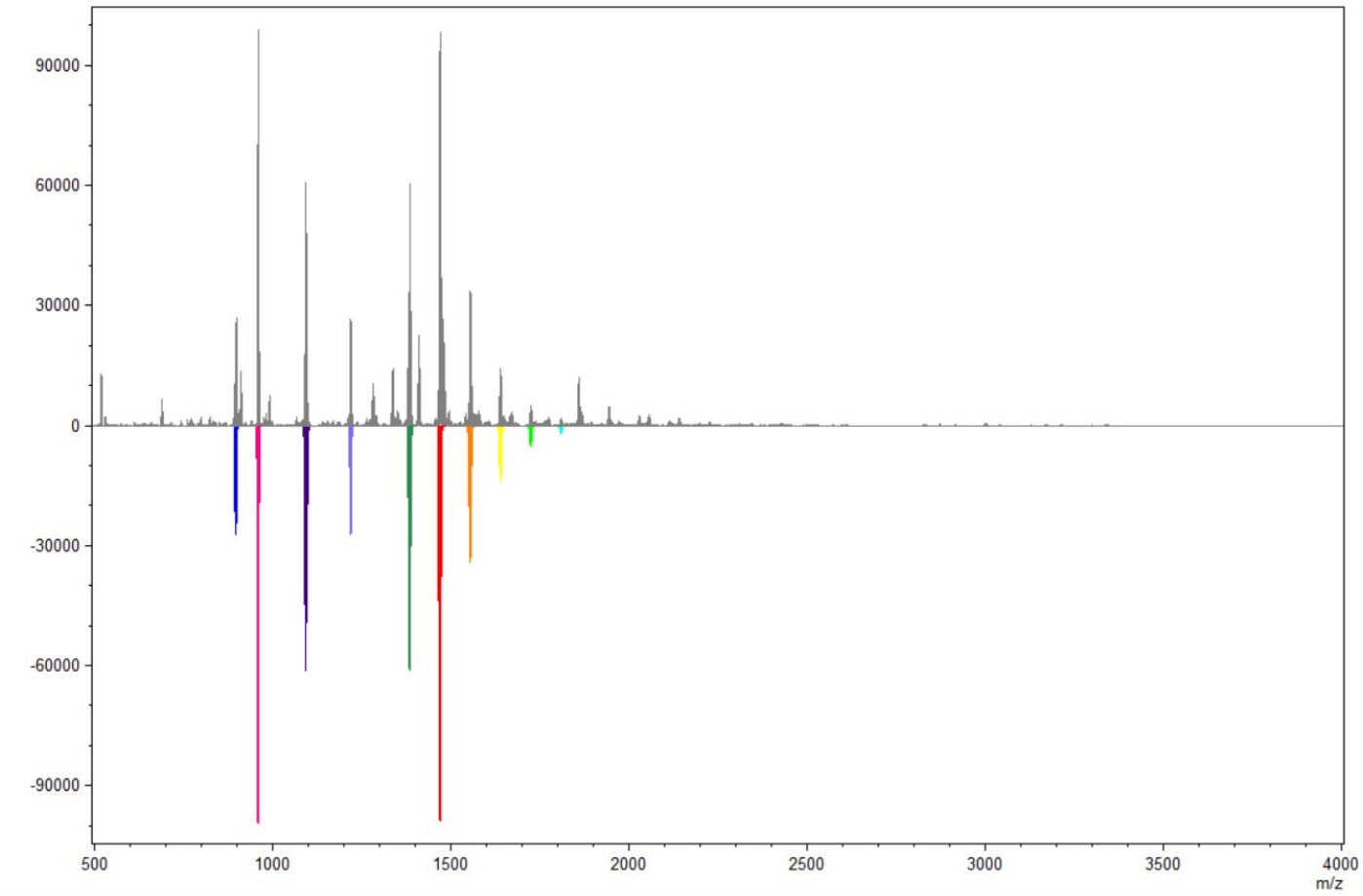

Table S11. Peak assignment for the spectrum of **3** presented in Fig. S27.

cation	m/z exp	m/z calc
$[Ag_{10}(C_4H_9S)_8]^{2+}$	896.193	896.195
$[Ag_{16}(C_4H_9S)_{12}(Br)]^{3+}$	958.633	958.634
$[Ag_6(C_4H_9S)_5]^{+}$	1092.638	1092.641
$[Ag_{20}(C_4H_9S)_{15}(Br)_2]^{3+}$	1218.189	1218.189
$[Ag_7(C_4H_9S)_6]^{+}$	1290.584	1290.588
$[Ag_{15}(C_4H_9S)_{12}Br]^{2+}$	1384.002	1384.001
$[Ag_{16}(C_4H_9S)_{12}(NO_3)Br]^{2+}$	1468.944	1468.946
$[Ag_{17}(C_4H_9S)_{12}(NO_3)_2Br]^{2+}$	1553.896	1553.894
$[Ag_{18}(C_4H_9S)_{12}(NO_3)_3Br]^{2+}$	1638.834	1638.839
$[Ag_{19}(C_4H_9S)_{12}(NO_3)_4Br]^{2+}$	1723.792	1723.786
$[Ag_{20}(C_4H_9S)_{12}(NO_3)_5Br]^{2+}$	1808.732	1808.731

Fig. S28. The comparison of observed and calculated isotopic patterns for the spectrum of **3** presented in Fig. S27.

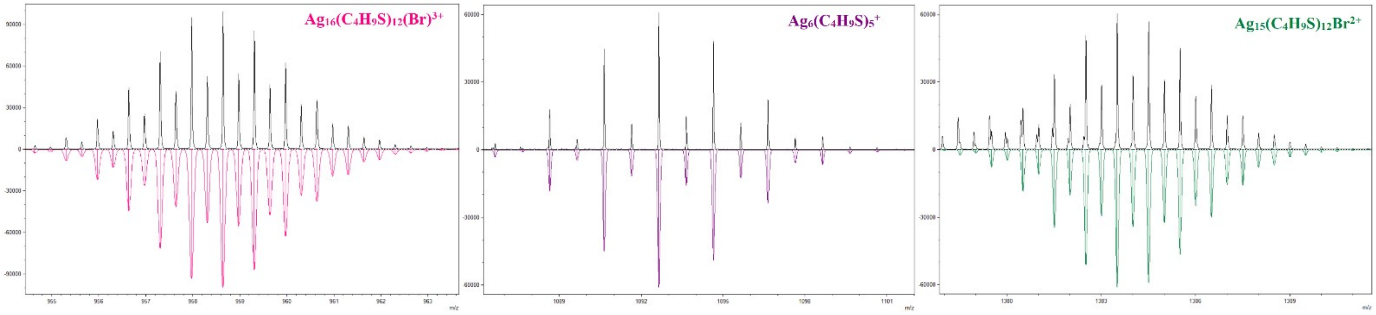

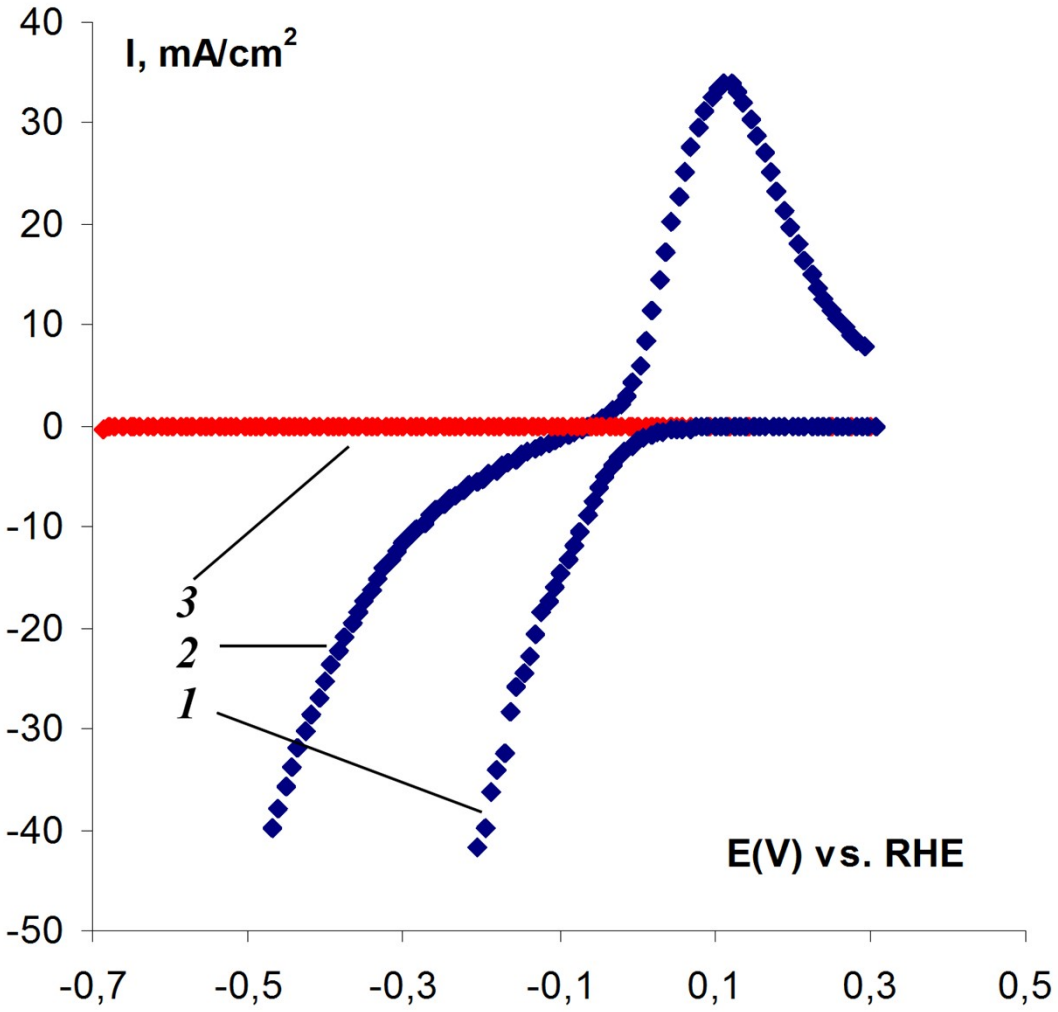

Fig. S29. Linear potential sweep (LRS) in the cathode region with **m-Ag_2S** material fixed on the surface (1), Ag2S (2), blank 0.5 M H_2SO_4 solution (3).

Degradation

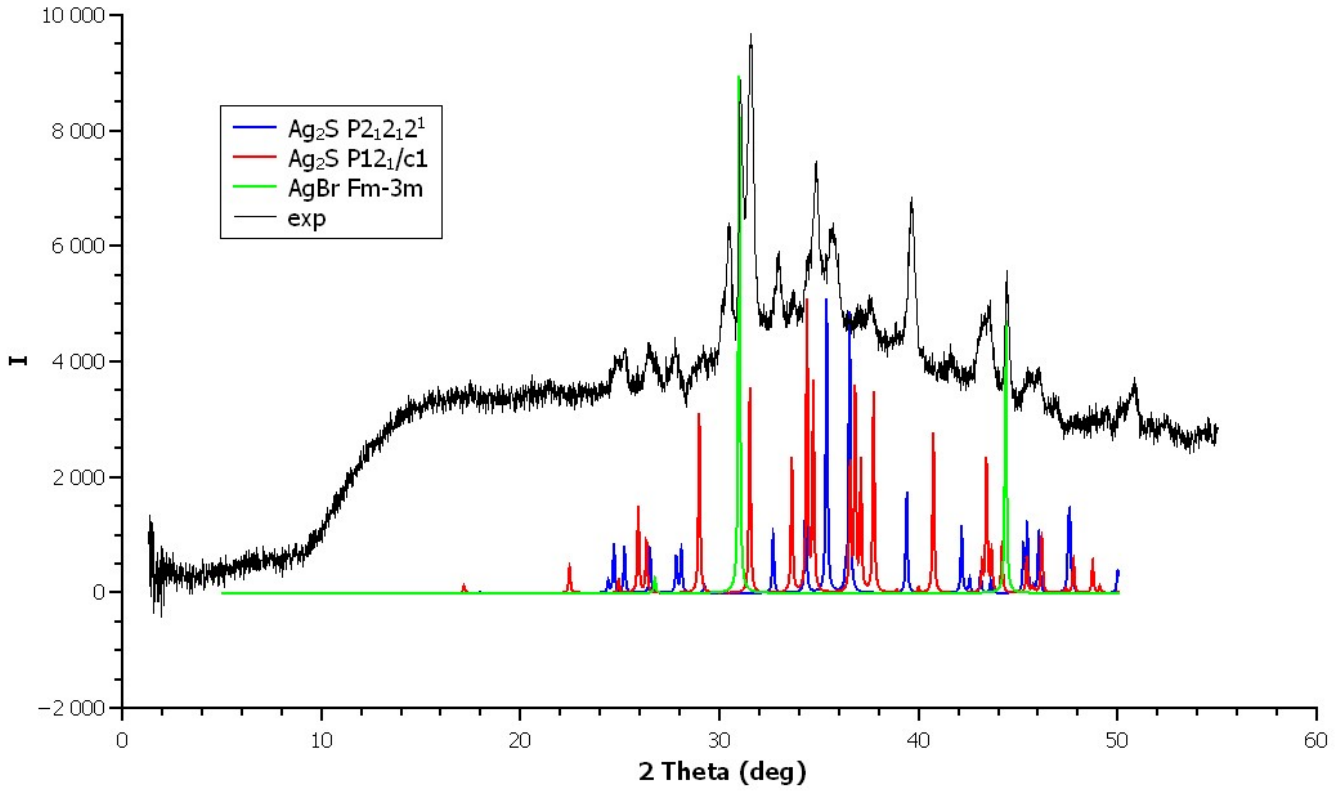

Fig. S30. XRPD of **m-Ag_2S**.

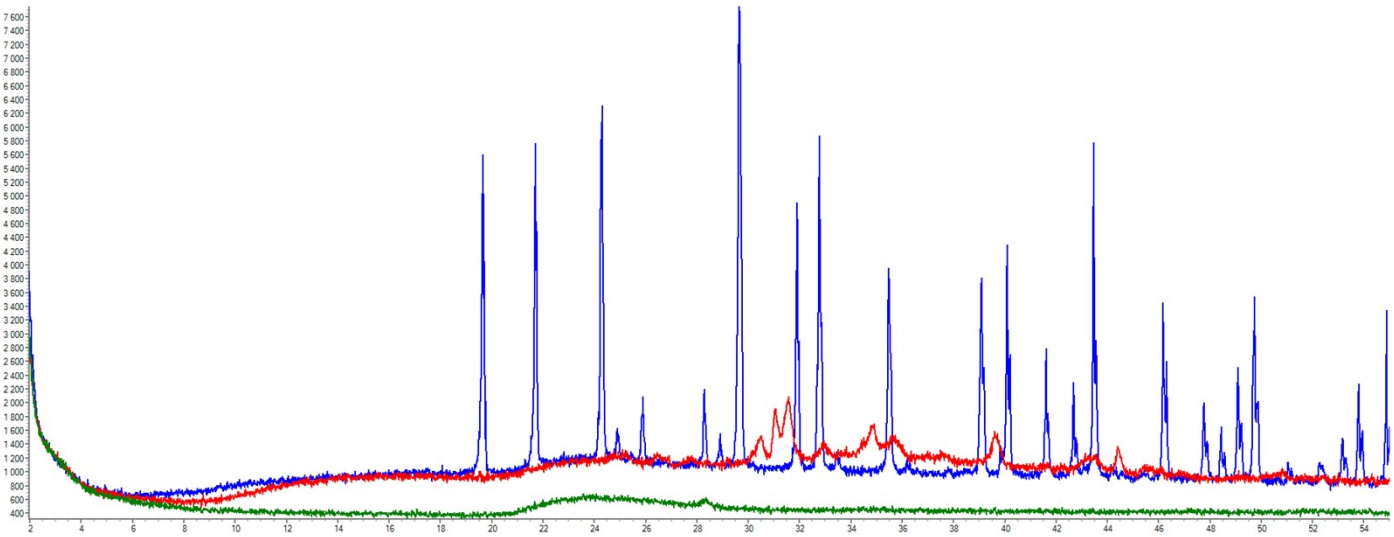

Fig. S31. XRPD patterns of **m-Ag_2S** (red), $AgNO_3$ (blue) and holder (green).

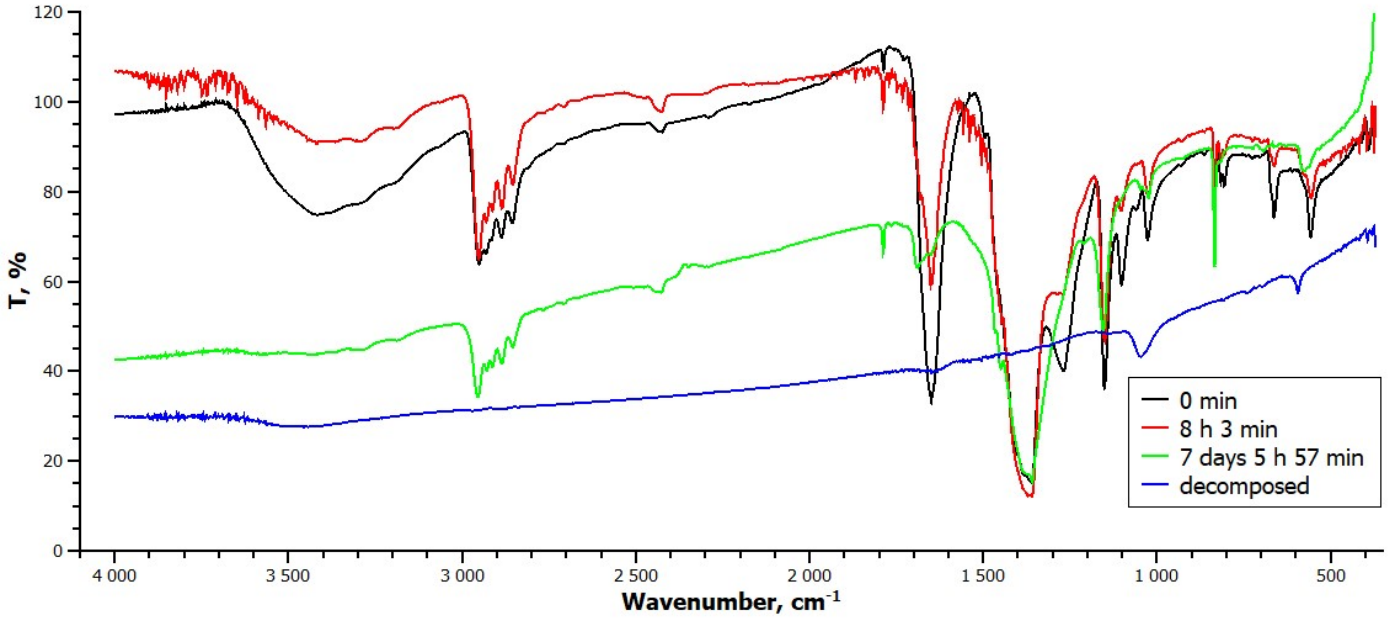

Fig. S32. The comparison of FTIR spectra during the decomposition of **3**.

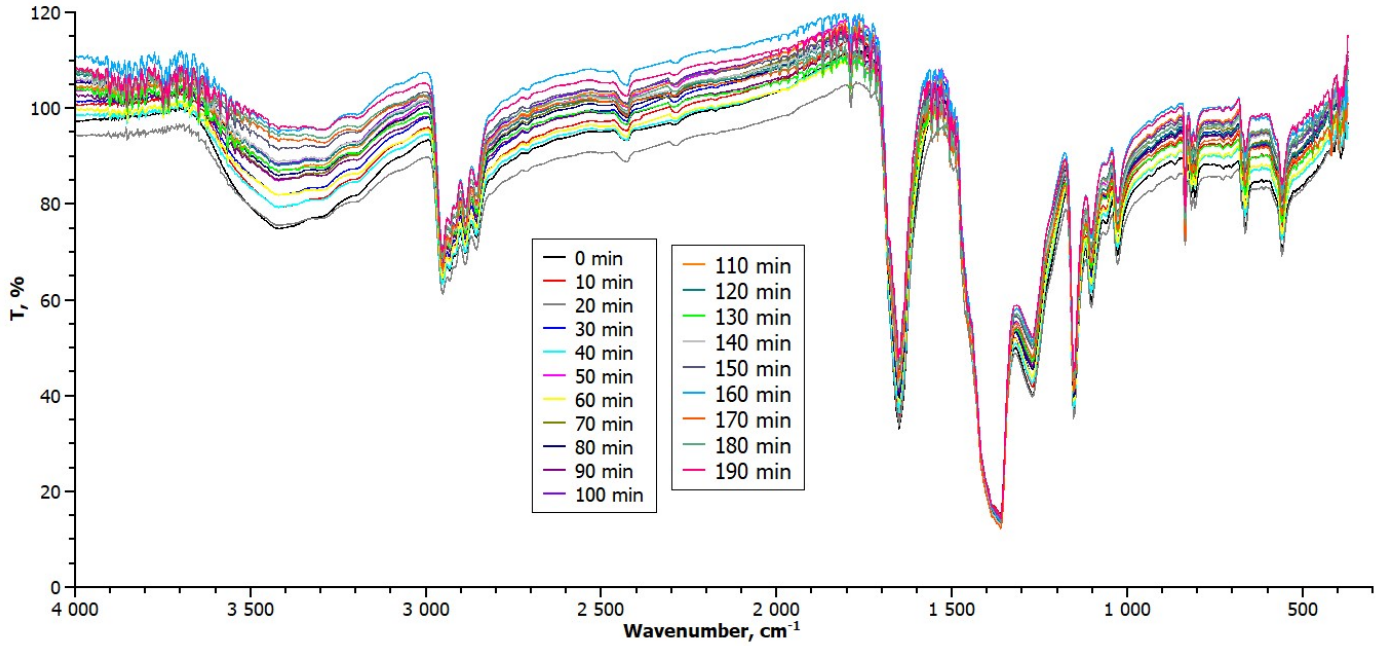

Fig. S33. The degradation of **3** in KBr pellet monitoring with FTIR.

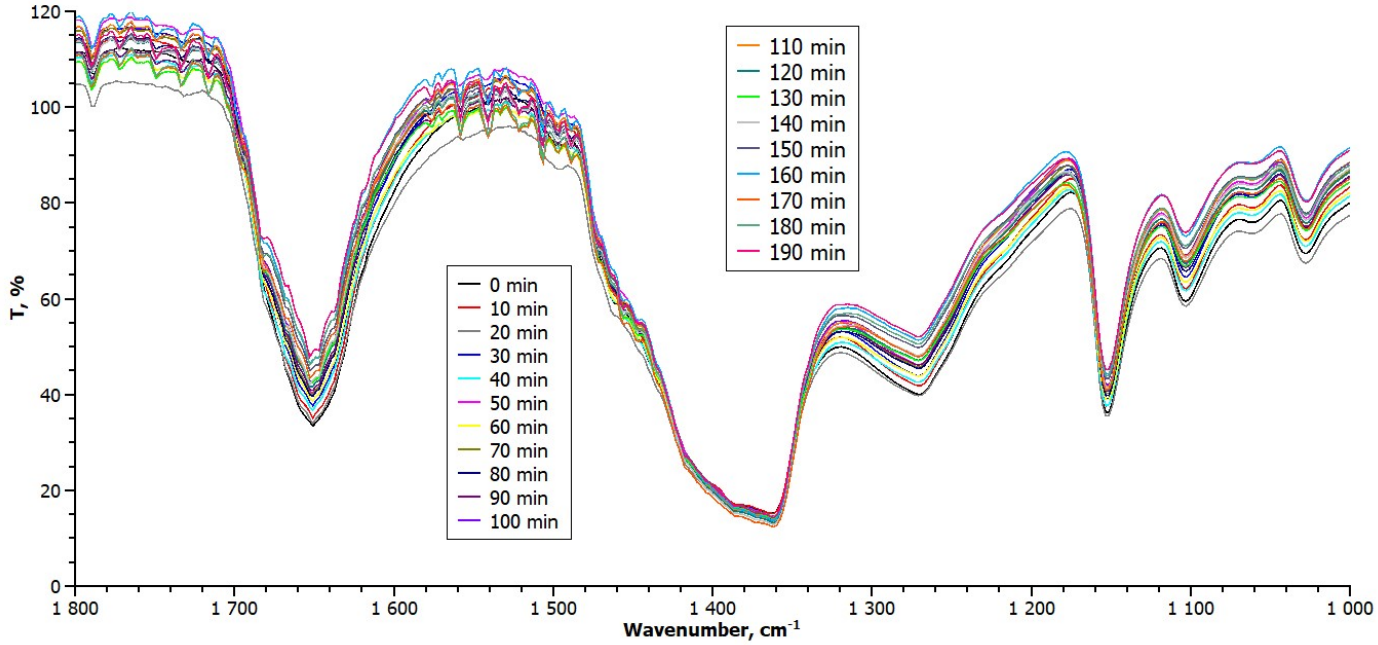

Fig. 34. The degradation of **3** in KBr pellet monitoring with FTIR (zoom 1800 – 1000 cm^{-1}).

Microscopy

Surface morphology observation was carried out using a field-emission scanning electron microscope JEOL JSM 6700F (Jeol, Japan). The determination of elemental composition was studied with a Quantax 200 (Bruker, Germany) analyzer for X-ray energy dispersive spectroscopy (EDX).

The results of EDX analysis carried out at various points revealed that the sample contains elements, the characteristic spectra of which are shown in Fig. S29, and detailed information on their quantitative content is presented in Tables S12, S13.

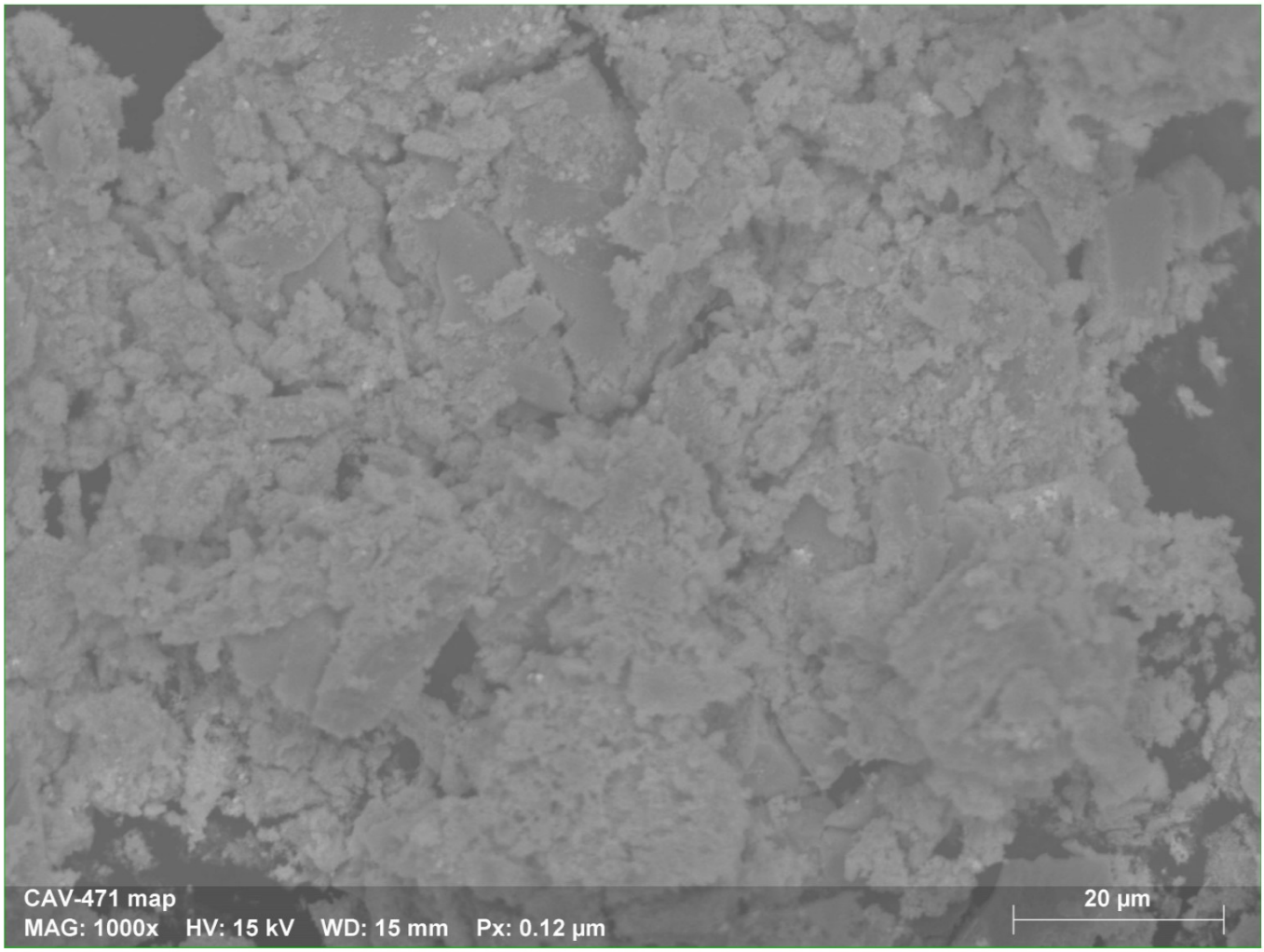

Fig. S35. SEM-image of **m-Ag_2S** sample surface morphology.

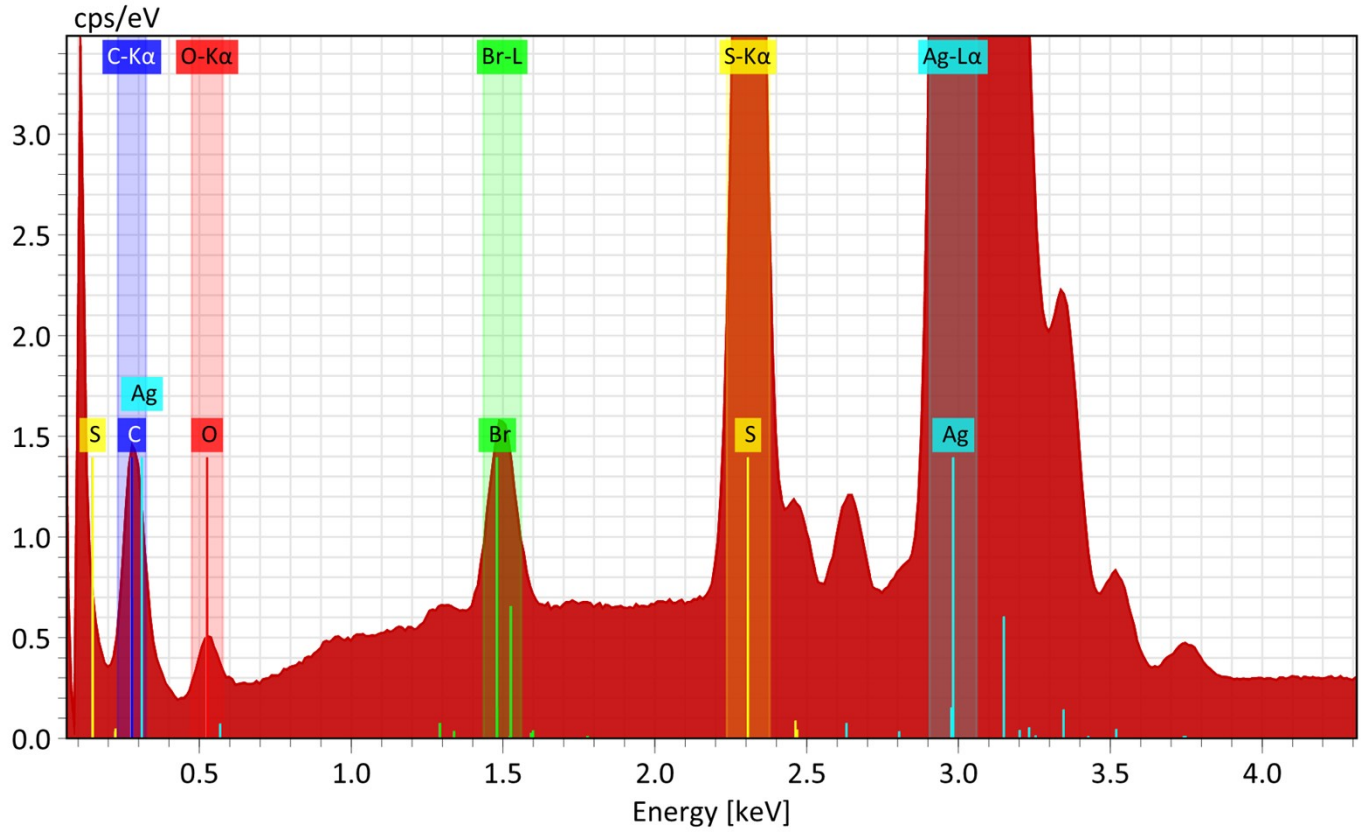

Fig. S36. Energy dispersive spectra for sample presented in Fig. S35.

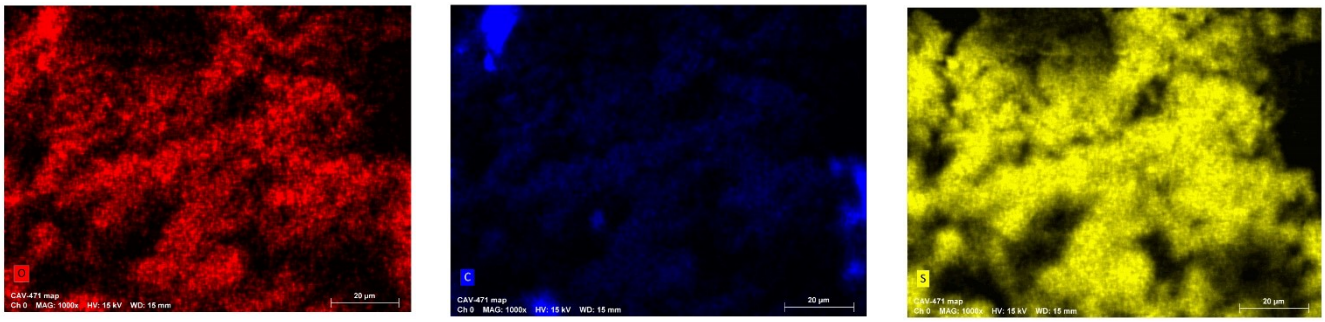

Fig. S37. EDX-mapping of the sample from Fig. S35.

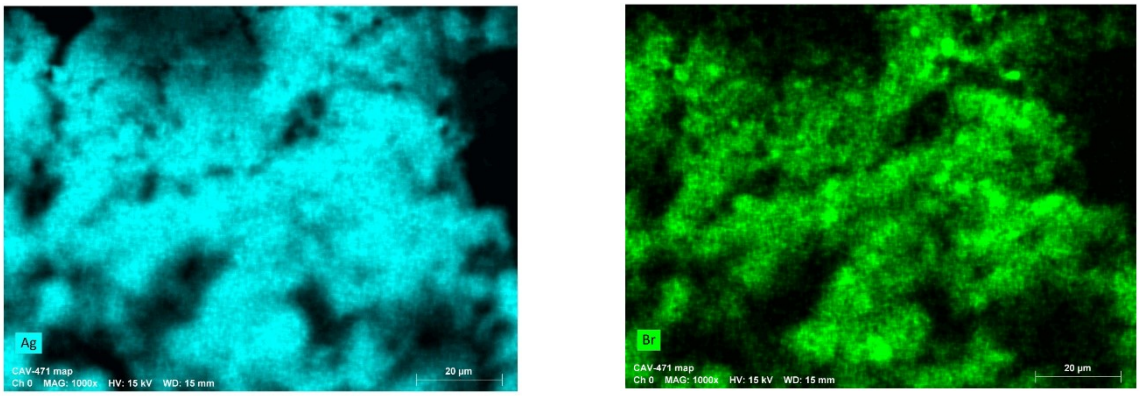

Table S12. Elemental composition of the sample.

Element	At. No.	Netto	Mass [%]	Mass Norm. [%]	Atom [%]	abs. error [%] (1 sigma)	rel. error [%] (1 sigma)
Oxygen	8	19439	2.49	2.28	9.33	0.35	13.87
Carbon	6	48969	3.54	3.24	17.65	0.44	12.51
Sulfur	16	623414	11.62	10.65	21.70	0.43	3.74
Silver	47	2543107	88.73	81.29	49.25	2.79	3.15
Bromine	35	77706	2.76	2.53	2.07	0.15	5.58
		Sum	**109.15**	**100.00**	**100.00**		

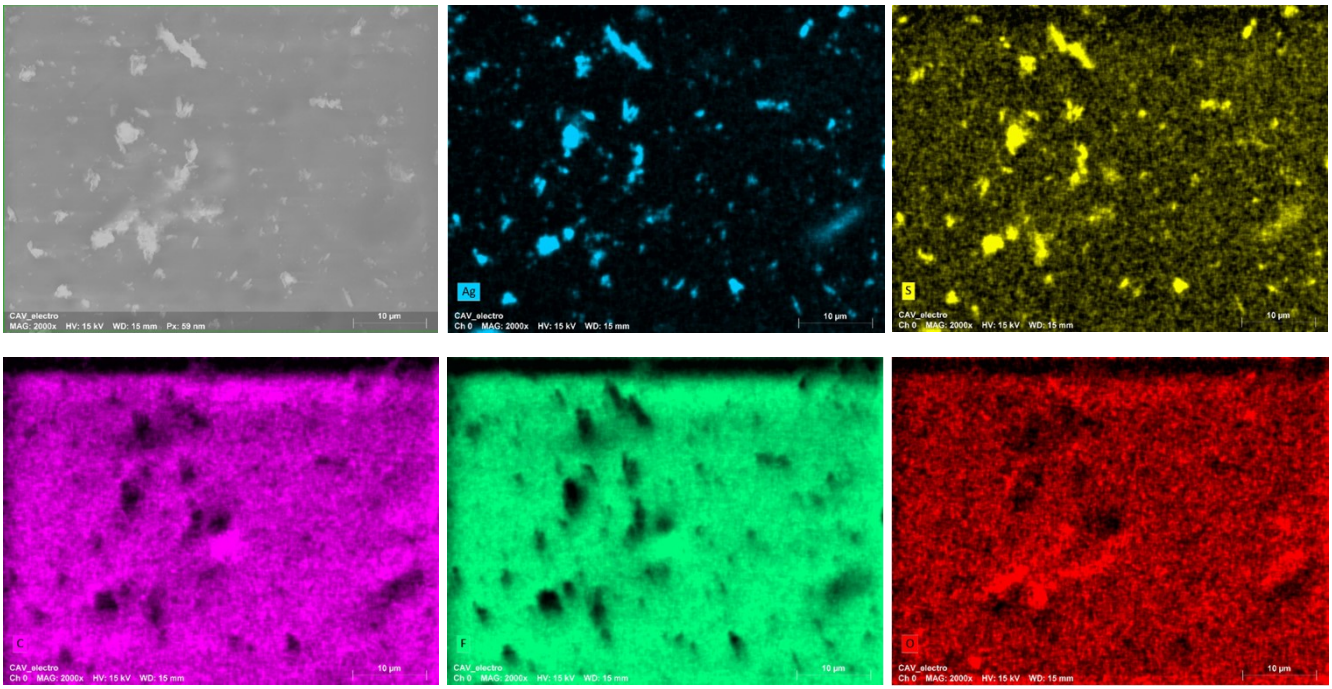

Fig. S38. EDX-mapping of the **m-Ag_2S-cat** sample from Fig. 7b.

Table S13. Elemental composition of the sample from Fig. 7b.

Element	At. No.	Netto	Mass [%]	Mass Norm. [%]	Atom [%]	abs. error [%] (1 sigma)	rel. error [%] (1 sigma)
Carbon	6	539028	27.61	27.61	38.87	2.94	10.64
Oxygen	8	61819	2.18	2.18	2.30	0.28	12.76
Sulfur	16	254079	2.76	2.76	1.46	0.12	4.44
Silver	47	176100	3.64	3.64	0.57	0.14	3.82
Fluorine	9	3023961	63.81	63.81	56.80	6.55	10.27
		Sum	**100.00**	**100.00**	**100.00**		

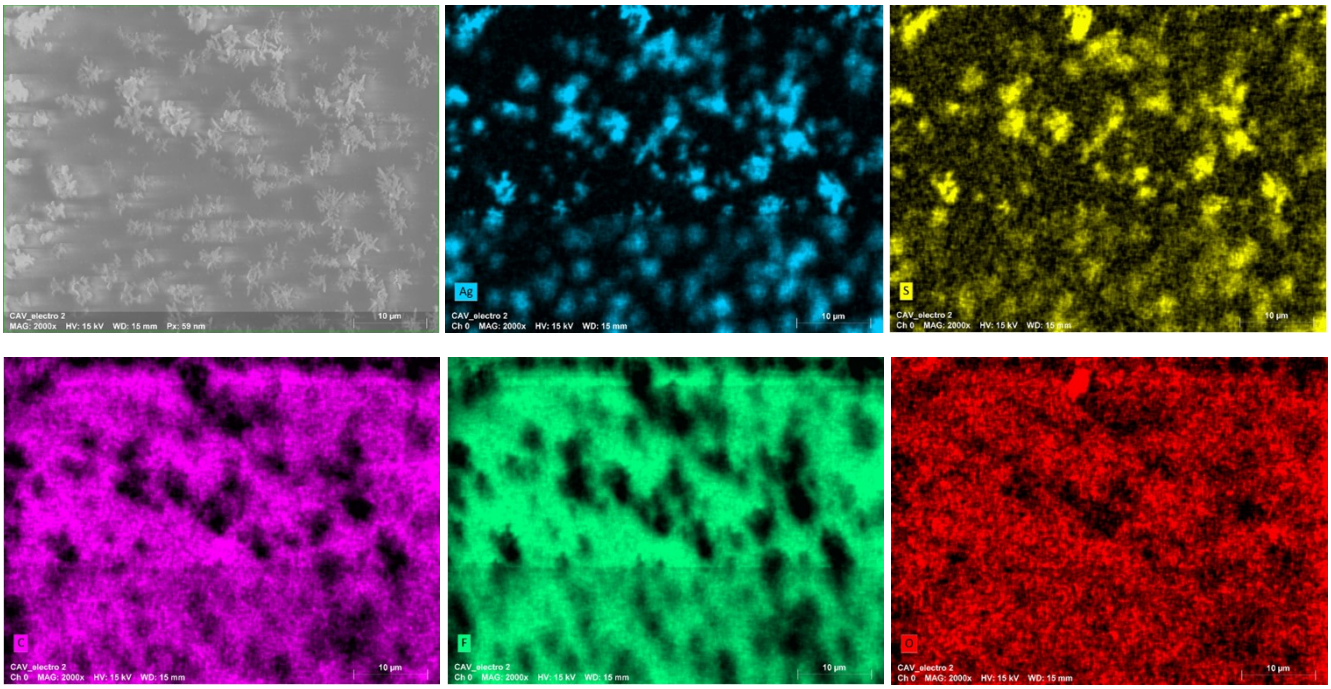

Fig. S39. EDX-mapping of the **m-Ag_2S-cat** sample from Fig. 7c.

Table S14. Elemental composition of the sample from Fig. 7c.

Element	At. No.	Netto	Mass [%]	Mass Norm. [%]	Atom [%]	abs. error [%] (1 sigma)	rel. error [%] (1 sigma)
Carbon	6	526876	24.32	26.19	38.26	2.59	10.65
Oxygen	8	50368	1.74	1.88	2.06	0.23	13.22
Sulfur	16	272398	2.78	2.99	1.64	0.12	4.43
Silver	47	342520	6.85	7.38	1.20	0.24	3.49
Fluorine	9	2736956	57.15	61.56	56.85	5.88	10.29
		Sum	**92.84**	**100.00**	**100.00**		

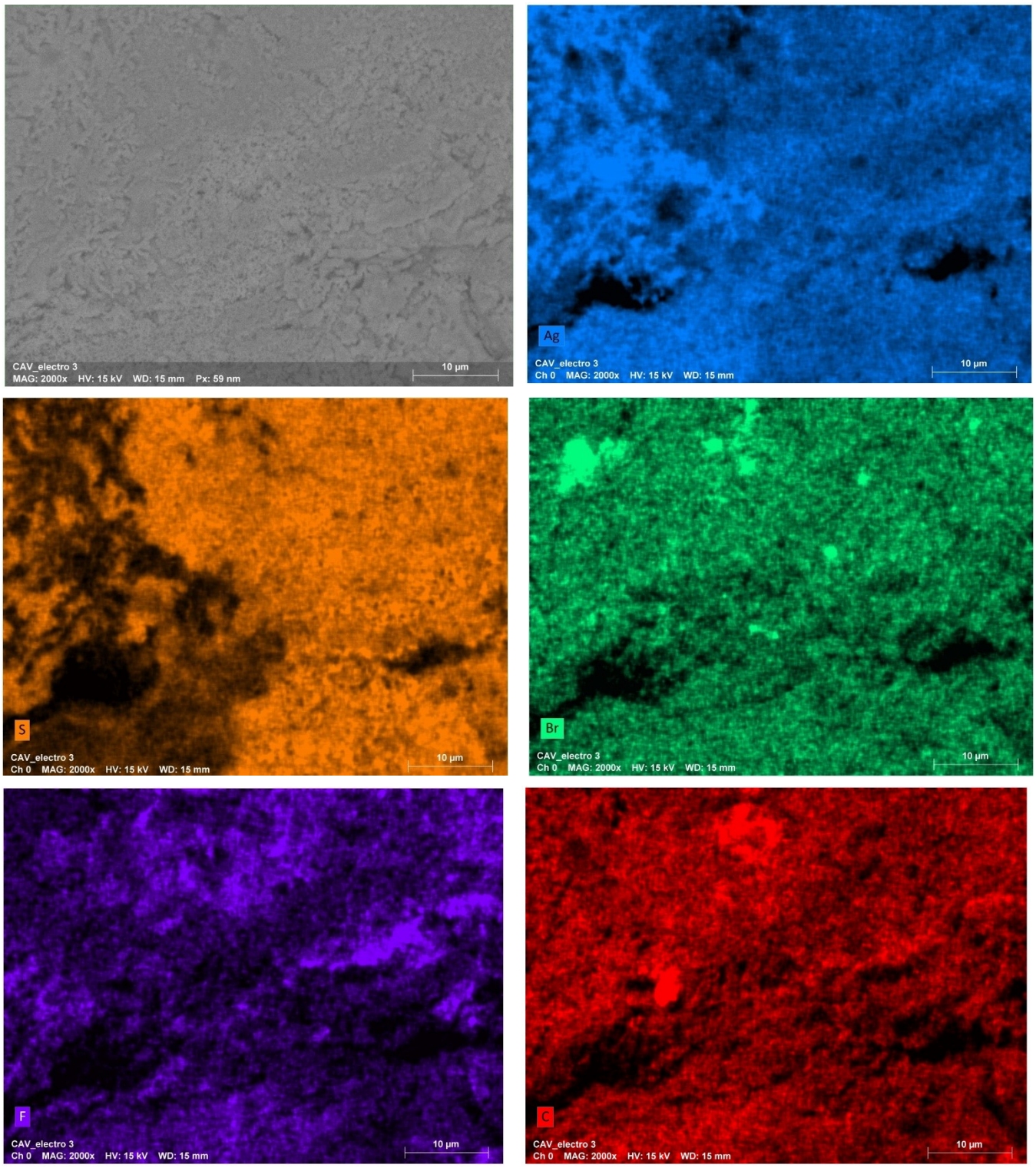

Fig. S40. A part of mapping for another area of **m-Ag_2S-cat**

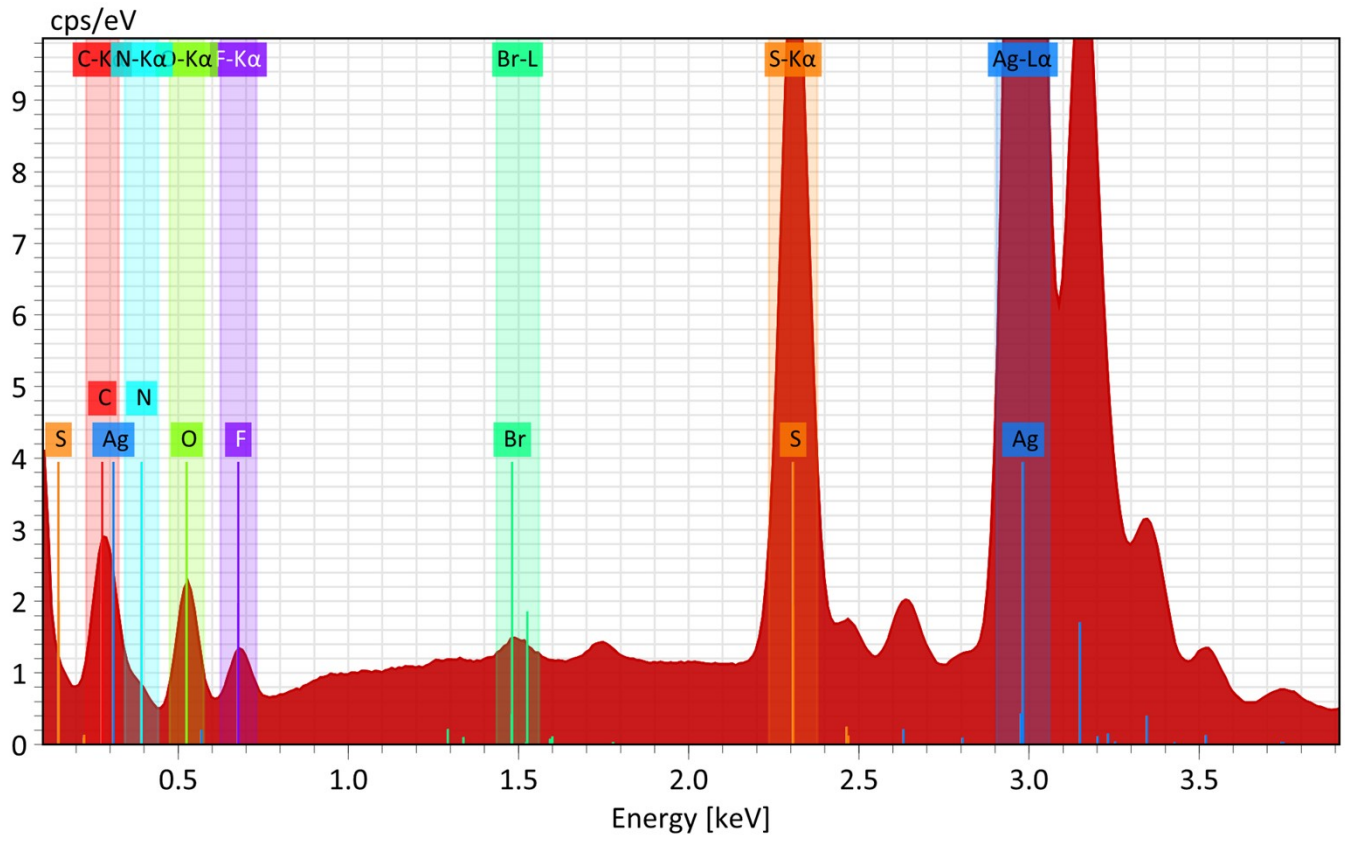

Fig. S41. Energy profile elemental analysis.

Element	At. No.	Netto	Mass [%]	Mass Norm. [%]	Atom [%]	abs. error [%] (1 sigma)	rel. error [%] (1 sigma)
Silver	47	3673990	73.48	74.37	33.80	2.32	3.15
Sulfur	16	884249	9.40	9.51	14.54	0.36	3.79
Bromine	35	17038	0.32	0.32	0.20	0.04	12.62
Fluorine	9	51847	2.67	2.70	6.97	0.34	12.69
Carbon	6	94026	3.56	3.60	14.71	0.43	12.01
Oxygen	8	113021	7.83	7.93	24.29	0.90	11.51
Nitrogen	7	22261	1.55	1.57	5.48	0.22	14.30
		Sum	**98.81**	**100.00**	**100.00**		

Table S15. Elemental composition of the sample.